Queen Mary
University of London
Science and Engineering

Radiation Detectors (SPA 6309)

Lecture 20

Peter Hobson

Last revised 6 April 2020

What is this lecture about?

- CMS ECAL
  - Design and construction
  - Performance
  - Radiation damage

Key points from previous lecture

- Why tracking is important
- Measuring momentum in homogenous magnetic fields
- Measuring impact parameters
- Effects of multiple scattering on performance

CMS Case Study 1

The Lead Tungstate Electromagnetic Calorimeter of the Compact Muon Solenoid (CMS) experiment at the Large Hadron Collider (LHC), CERN

(With acknowledgements to CMS colleagues, particularly R M Brown at RAL but all errors and omissions are my responsibility)

The Compact Muon Solenoid

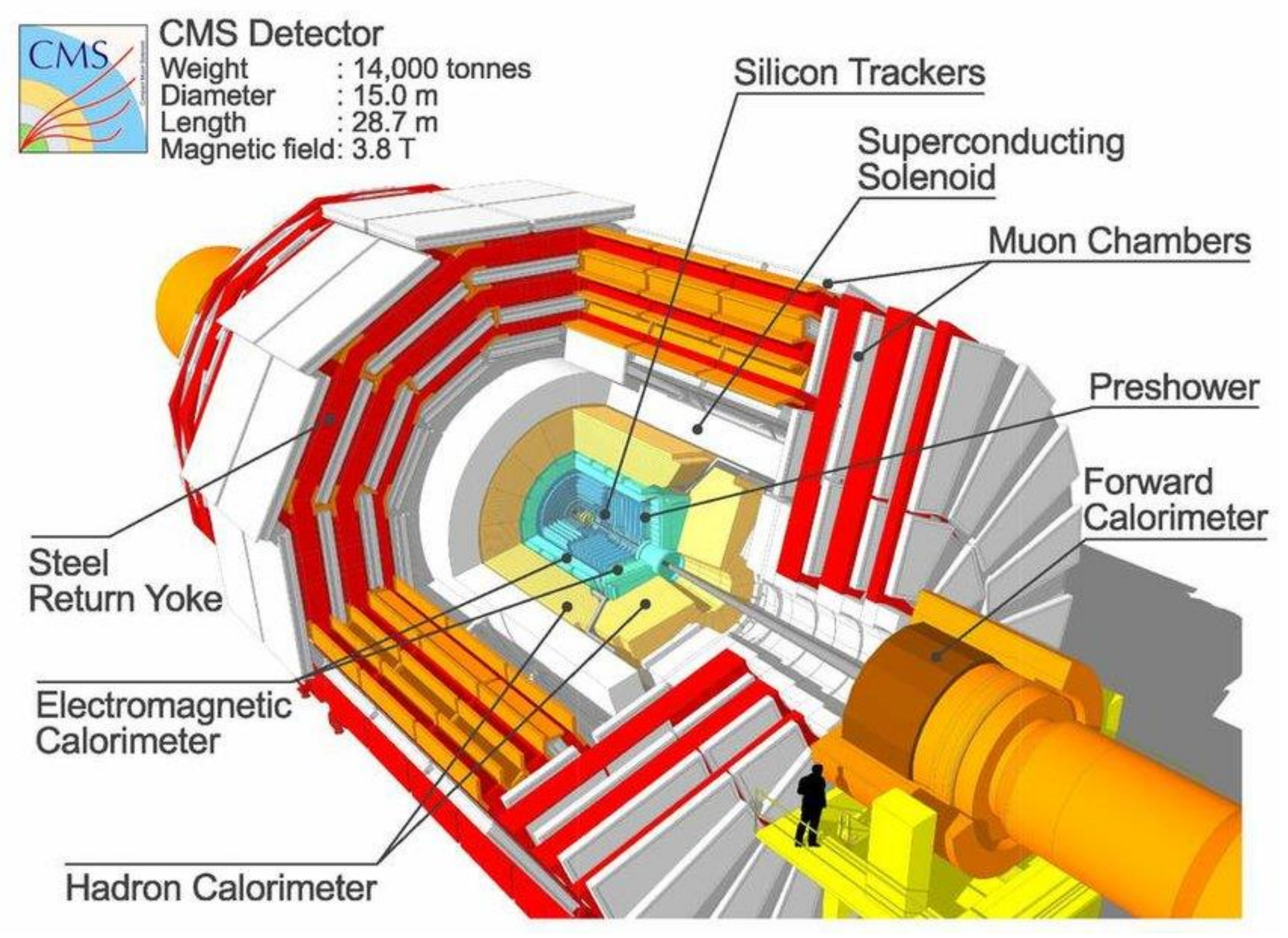

ECAL design objectives

High resolution electromagnetic calorimetry is a basic design objective of CMS

Benchmark physics process:

Sensitivity to a low mass Higgs via $H \to \gamma\gamma$

$$\sigma_m / m = 0.5 [\sigma_{E_1}/E_1 \oplus \sigma_{E_2}/E_2 \oplus \sigma_\theta / \tan(\theta/2)]$$

Where $\sigma_E/E = a/\sqrt{E} \oplus b \oplus c/E$

Aim:		Barrel	End cap
Stochastic term:	a =	2.7%	5.7%
(photoelectron statistics/shower fluctuations)			
Constant term:	b =	0.55%	0.55%
(non-uniformities, shower leakage)			
Noise term: Low $\mathcal{L}$	c =	155 MeV	205 MeV
High $\mathcal{L}$		210 MeV	245 MeV

(Angular resolution limited by uncertainty in position of interaction vertex)

Simulated Higgs to $\gamma\gamma$ events for 130 GeV Higgs (actually found to be 125.4 GeV/c^2)

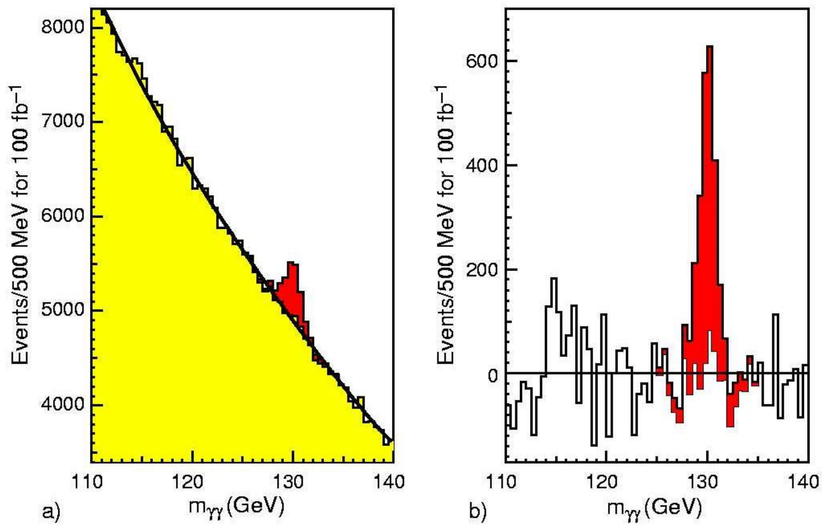

ECAL design choices

- ECAL (and HCAL) within magnetic volume
- Homogenous scintillator ($PbWO_4$)
- Magnetic field-tolerant photodetectors with gain:
  - Avalanche photodiode (APD) for barrel
  - Vacuum phototriode (VPT) for end caps
- Pb/Si Preshower detector in end caps

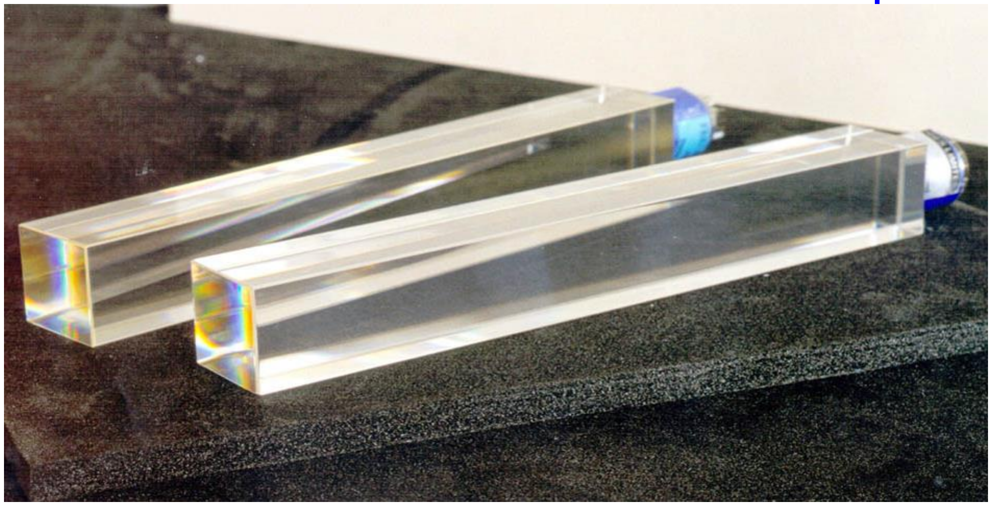

Properties of dense inorganic scintillators

Property	BGO	BaF_2	CeF_3	$PbWO_4$
Density [g/cm^3]	7.13	4.88	6.16	8.28
Rad length [cm]	1.12	2.06	1.68	0.89
Int length [cm]	21.8	29.9	26.2	22.4
Molière rad [cm]	2.33	3.39	2.63	2.19
Decay time [ns]	60 300	0.9 630	8 25	5(39%) 15(60%) 100(1%)
Refractive index	2.15	1.49	1.62	2.30
Max emiss [nm]	480	210 310	300 340	420
Temp coef [%/ºC]	-1.6	0 -2	0.14	-2
Rel light yield	18	4 20	8	1.3

ECAL Parameters

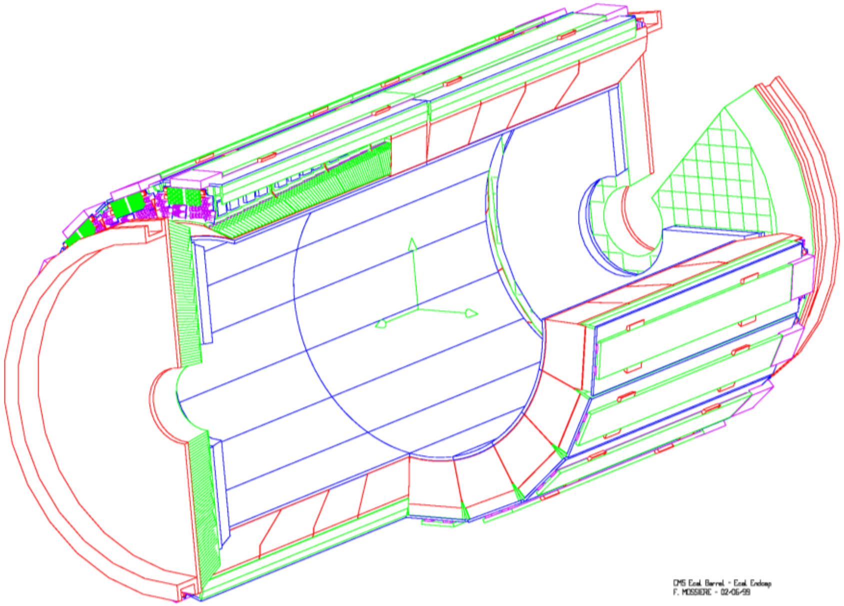

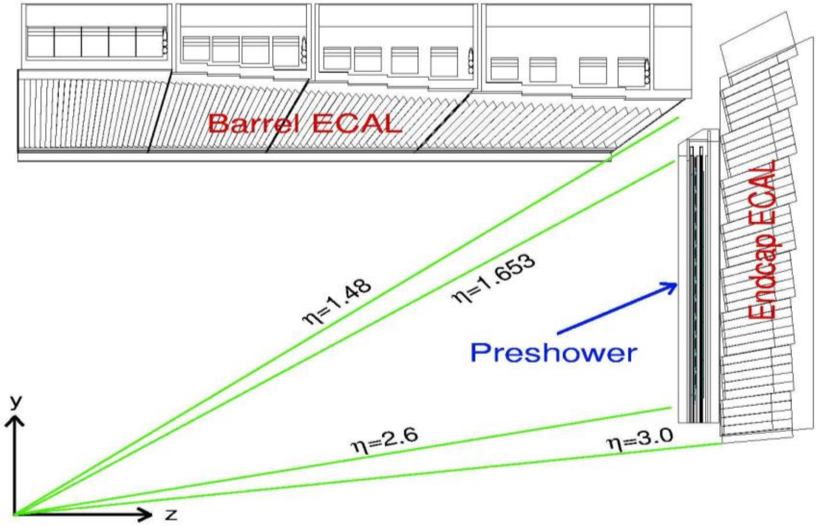

Parameter	Barrel	End caps
Coverage	$\lvert\eta\rvert < 1.48$	$1.48 < \lvert\eta\rvert < 3.0$
$\Delta\varphi \times \Delta\eta$	0.0175×0.0175	0.0175×0.0175 to 0.05×0.05
Xtal size (mm^3)	$21.8 \times 21.8 \times 230$	$30.0 \times 30.0 \times 220$
Depth in X_0	25.8	24.7
# of crystals	61200	14648
Volume (m^3)	8.14	2.7
Xtal mass (t)	67.4	22.0

3° off-pointing pseudo-projective geometry

Radiation levels in ECAL

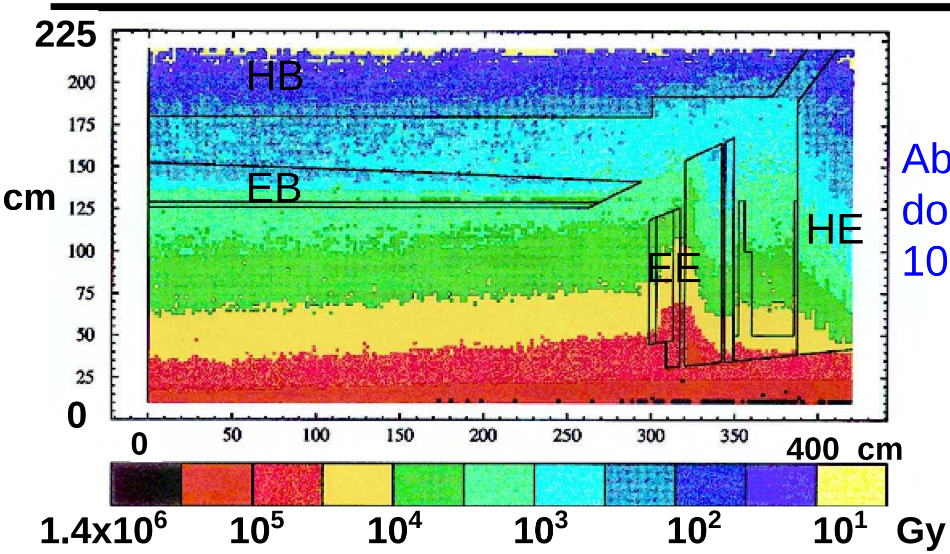

Absorbed dose after 10 years

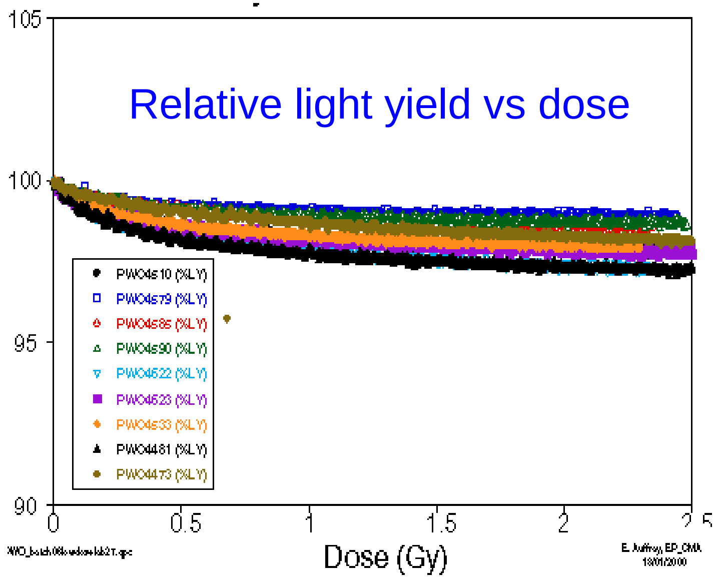

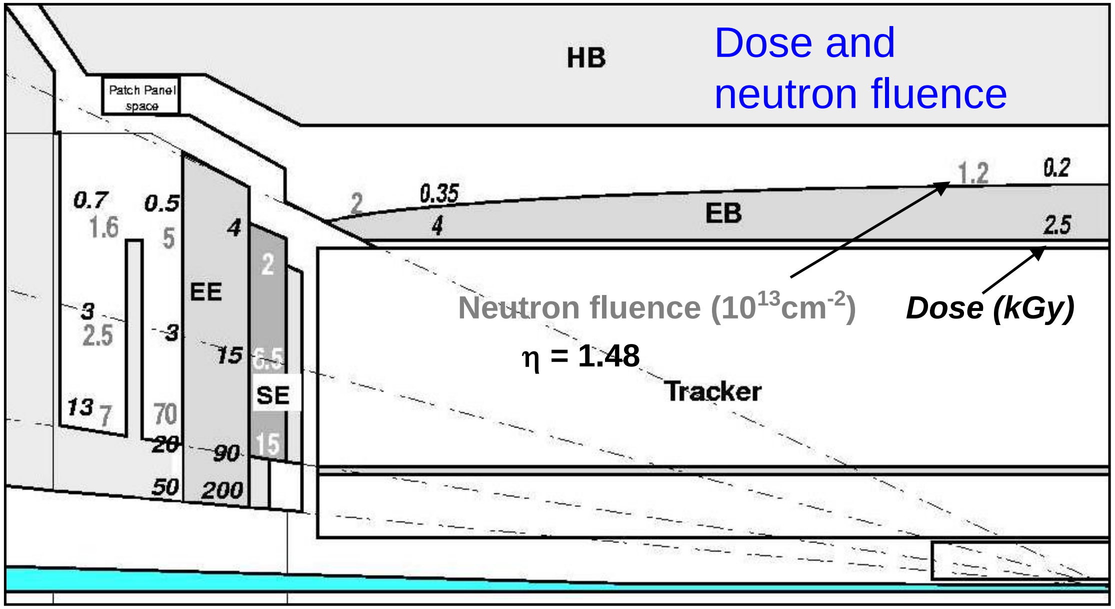

Effect of radiation on $PbWO_4$
(after intense R&D)

- No change in scintillation properties
- Small loss in transmission through formation of colour centres
- Damage saturates
- Slow self-annealing occurs
- Loss in light yield of a few percent corrected with monitoring system
- No damage observed with neutrons

BUT see later slides!

Photodetectors –solid state

- Silicon is the primary material since in general we are detecting fast scintillation or Cherenkov light (near UV to visible)
- Silicon diode technology is well advanced and the quantum efficiency (QE) is high (around 80% peak)
- Silicon devices are tolerant to quite high radiation levels, although there are problems with hadrons.
- Silicon photodiodes are linear over many orders of magnitude
- The *Avalanche Photodiode* has internal gain of about 30 (optimum value).
- See
  - https://www.hamamatsu.com/eu/en/product/optical-sensors/apd/si-apd/index.html

Photodetectors: barrel

Avalanche photodiodes (APD)

- Operated at a gain of 50
- Active area of 2 x 25mm^2/crystal
- Q.E. ~ 80% for $PbWO_4$ emission
- Excess noise factor is F = 2.2
- Insensitive to shower leakage particles (d_{eff} ~ 6 μm)
- Irradiation causes bulk leakage current to increase

➔ electronic noise doubles after 10 yrs - **acceptable**

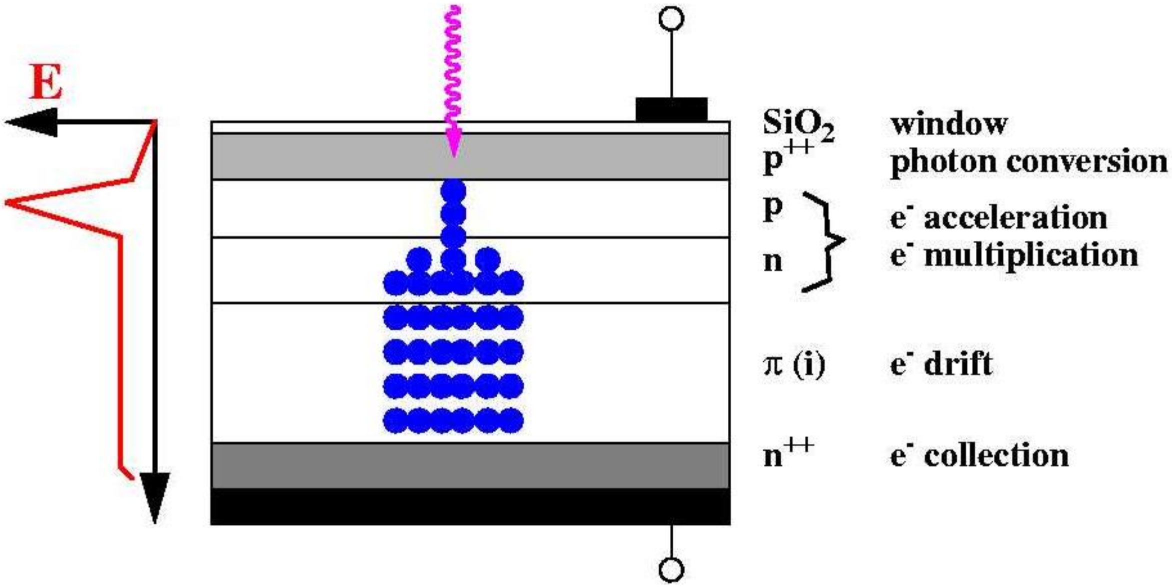

Hamamatsu APD

Hamamatsu type S8148

QE, Gain *vs* applied bias voltage, Excess Noise Factor

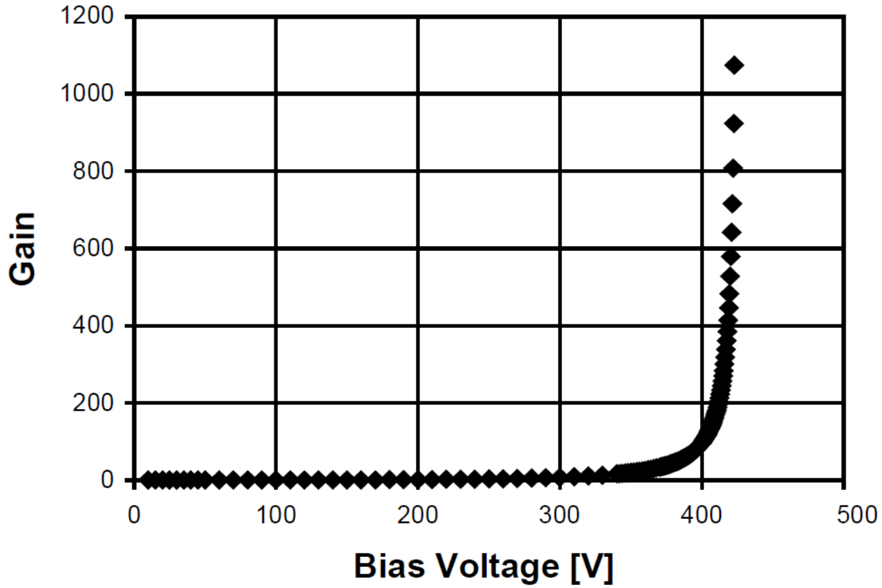

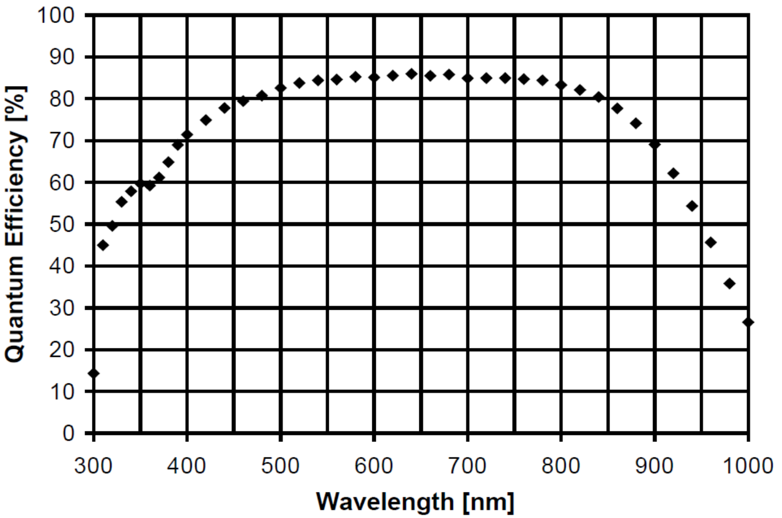

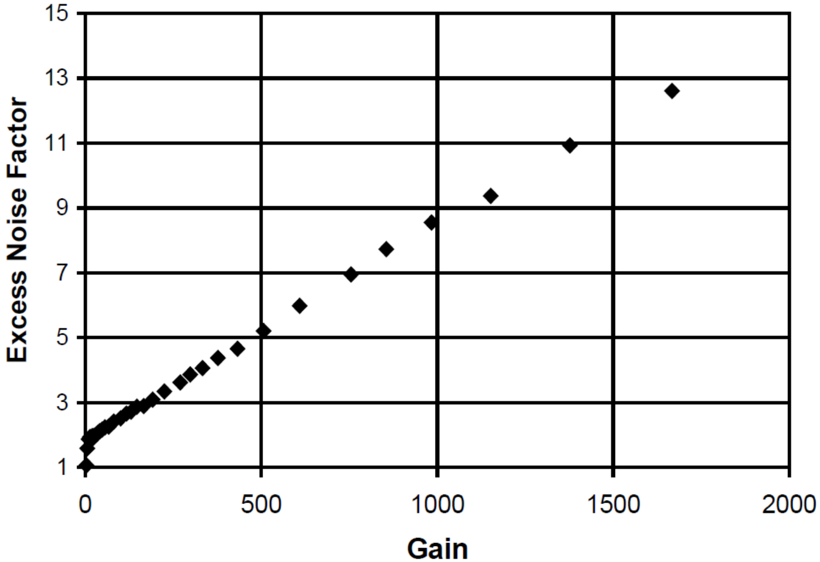

See D. Renker, *NIM A* 486 (2002) 164

Photodetectors –solid state

- Silicon is *not* cheaper per unit area than vacuum photodetectors (for areas greater than a few tens of mm^{2})
- Really large devices cannot be made (200 mm^2 is the upper limit) excluding solar cells of course.
- Problem of damage from high neutron flux in hadron collider experiments such as those at the LHC.
- Often need low noise pre-amplifiers.

Photodetectors: end caps

Endcaps: Vacuum phototriodes (VPT)

Produced by RIE, St Petersburg, Russia

More radiation resistant than Si diodes (with UV glass window)

- Active area ~ 280 mm^2
- Gain ~10 (B=4T) Q.E.~ 20% (420 nm)
- Fast devices (simple planar structure)

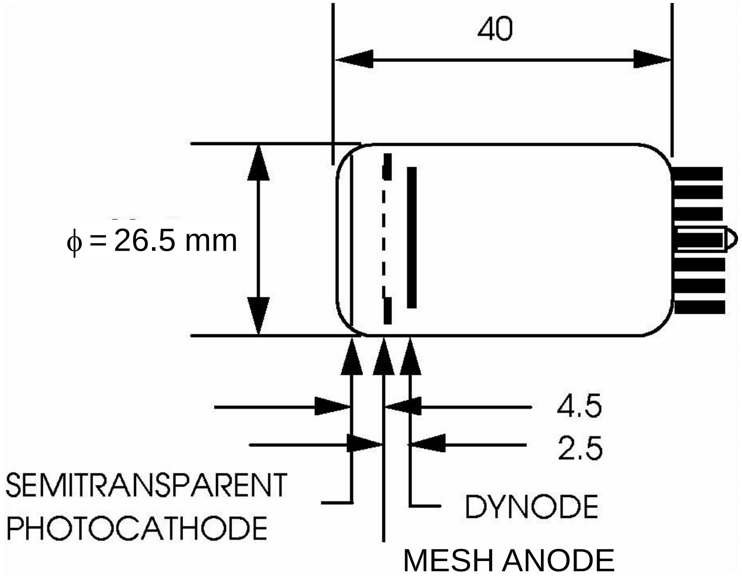

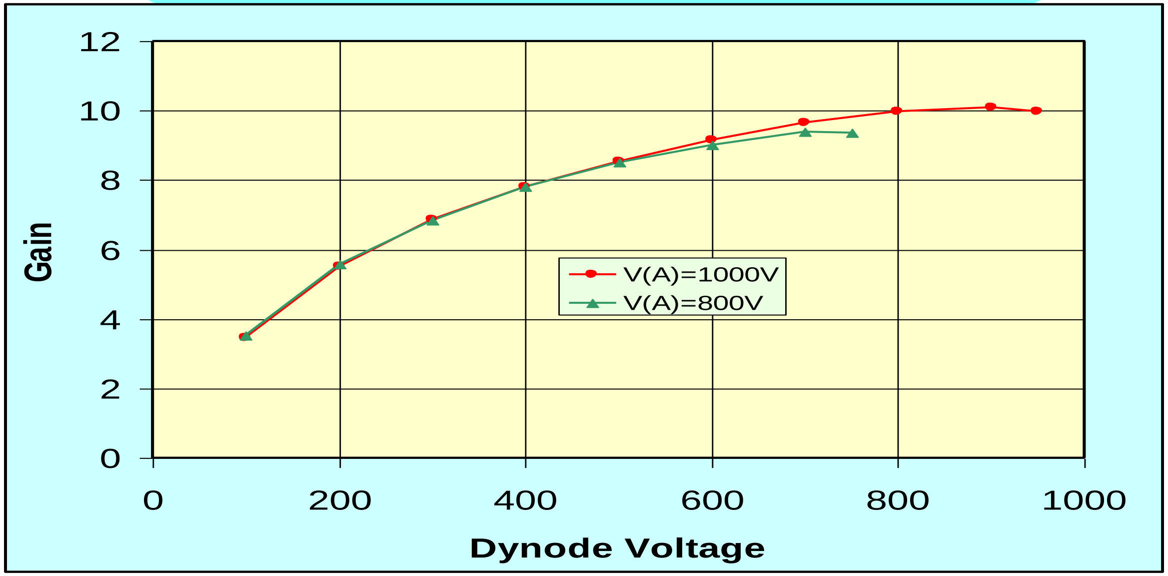

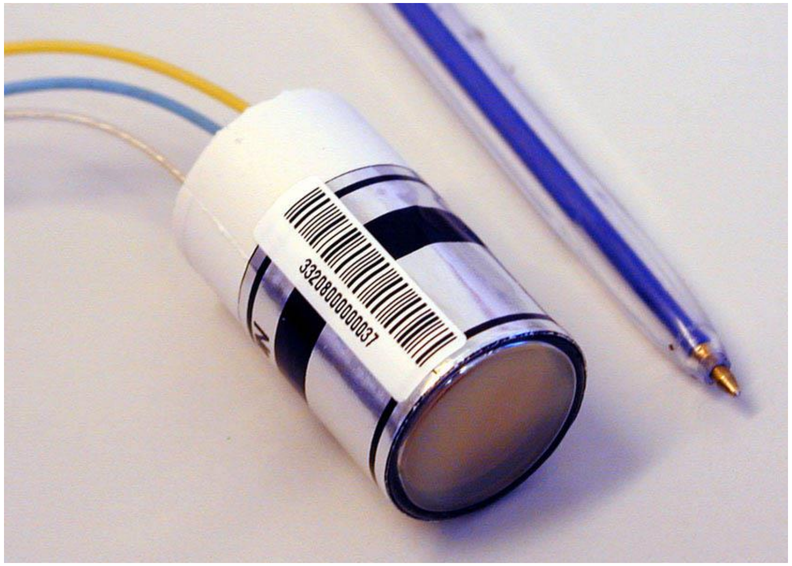

VPT Characteristics

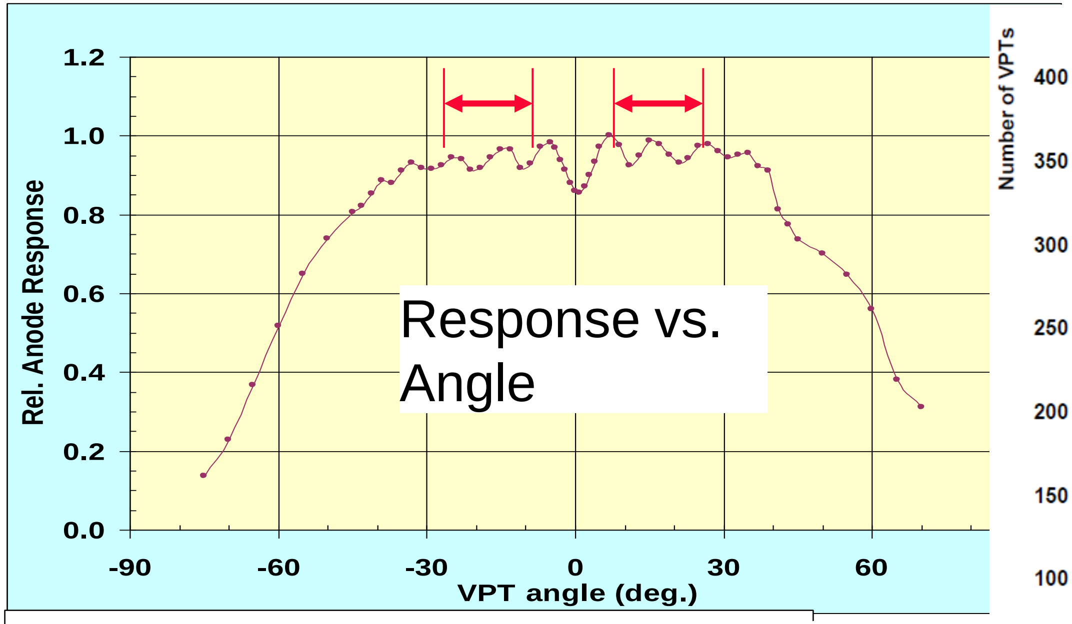

Response vs. Angle

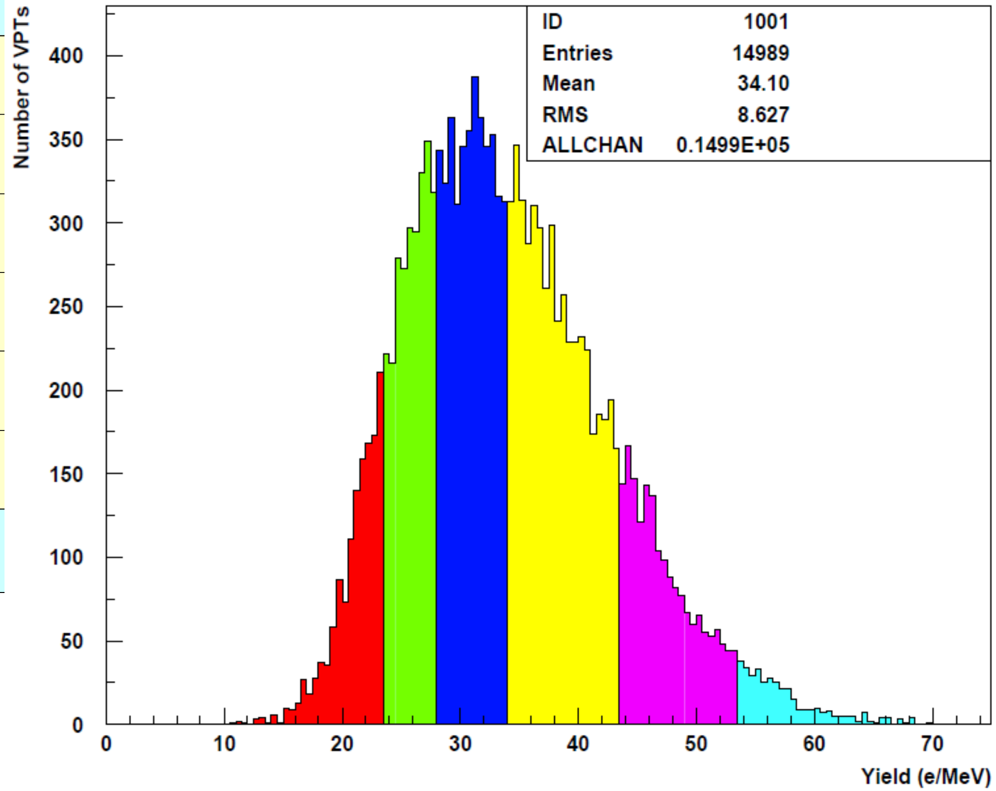

Only 8% loss of transparency after 20 kGy (10 years)

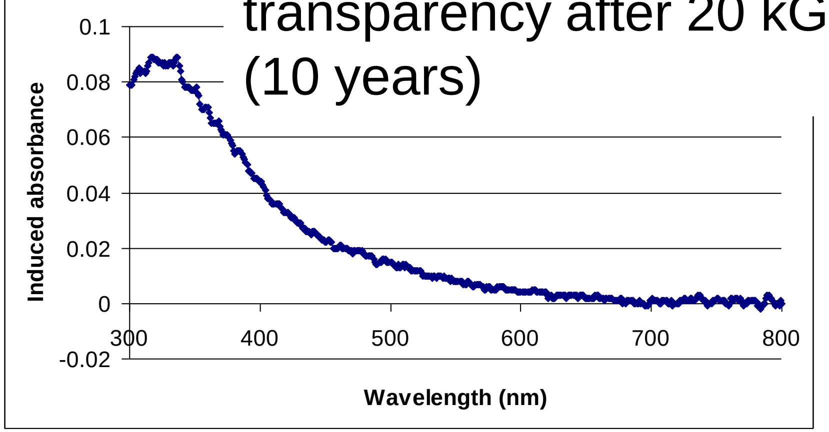

Critical magnetic field and radiation tolerance tests were done in the UK.

Construction: barrel

Submodule: 2x5 Xtals with APD and FE electronics in 200μm glass fibre alveola

Module: 10x4 or 10x5 submodules mounted on a 'Grid', inside a 'basket'

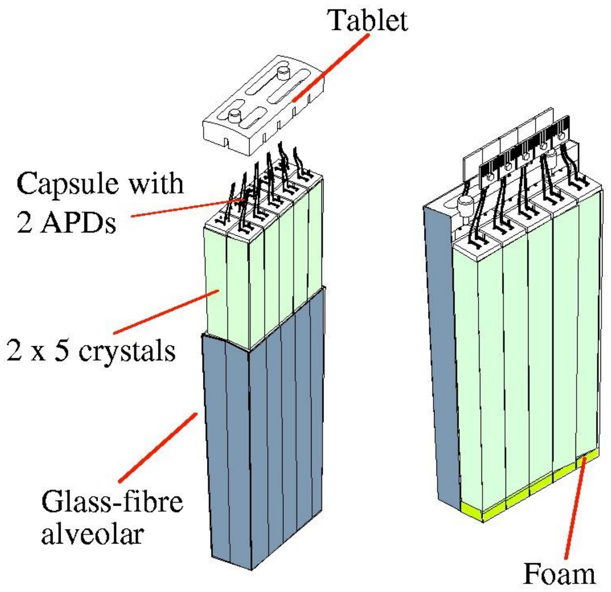

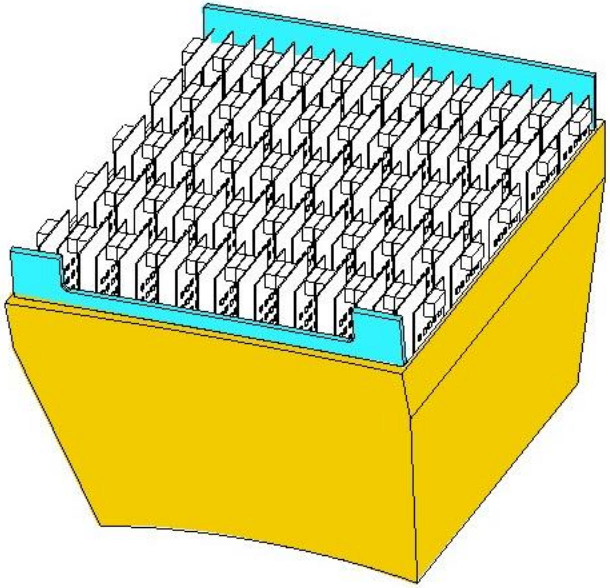

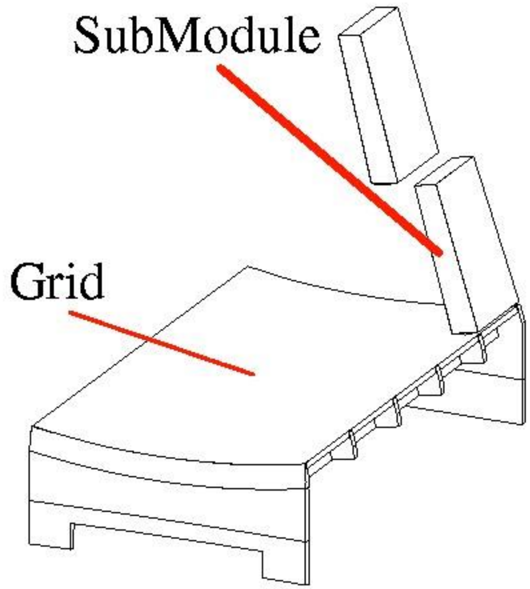

Assembled Submodules

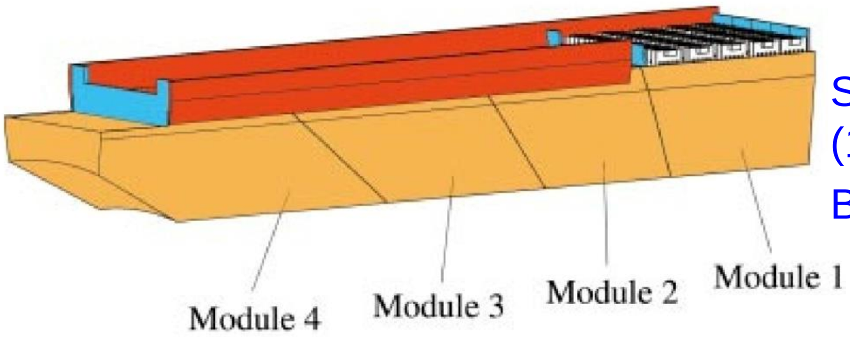

Supermodule: 4 Modules (1700 Xtals)

Barrel = 36 Supermodules

Construction: end caps

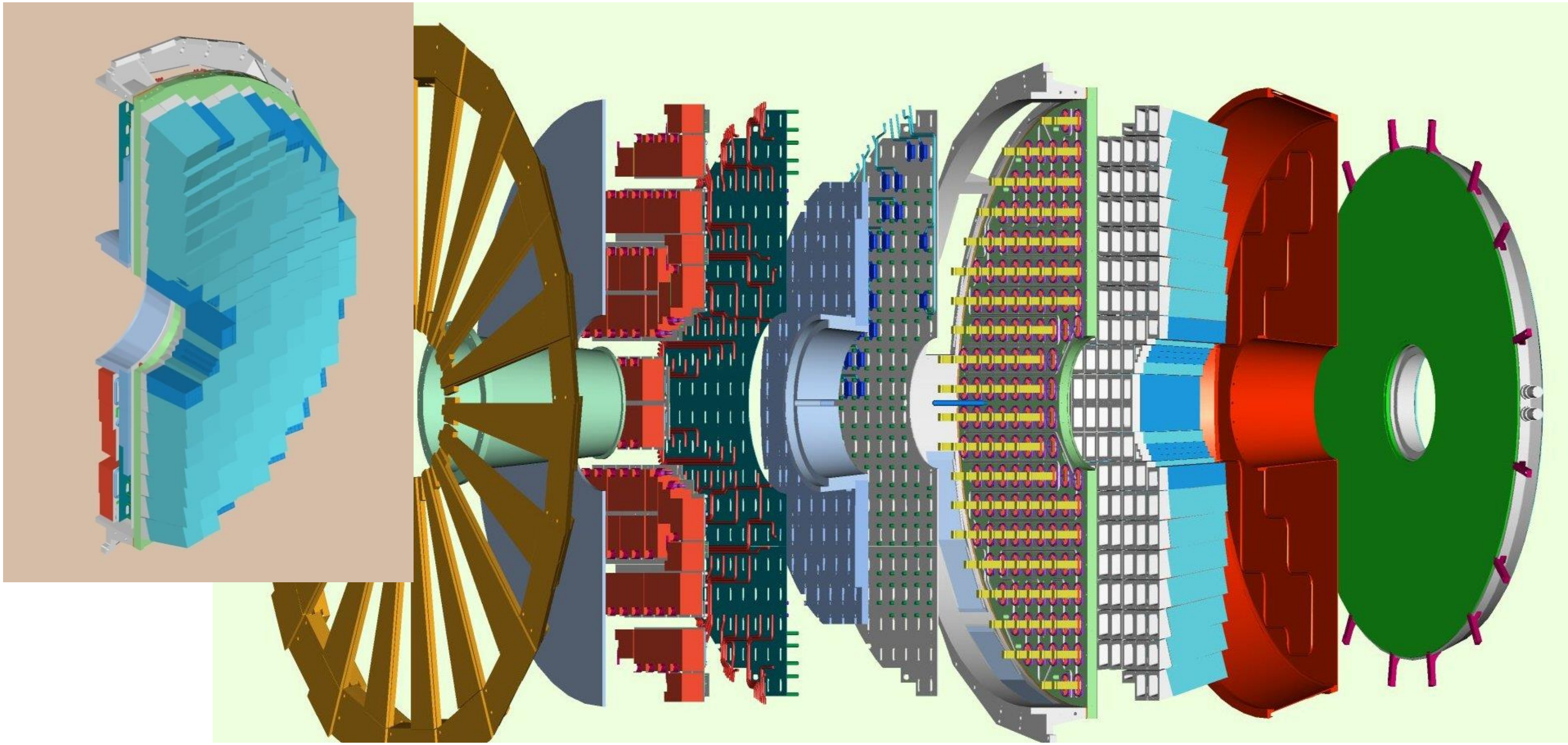

The endcap is mechanically complex

Tight tolerance on dimensions, deflections and thermal management.

Construction: end caps

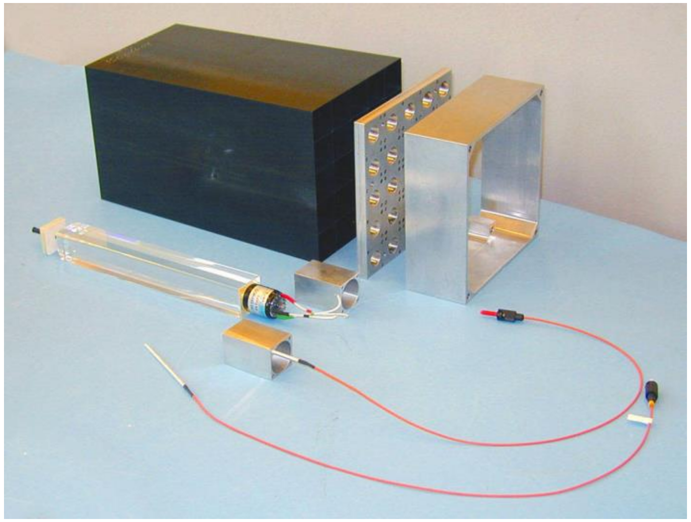

'**Supercrystal**': carbon-fibre alveola containing 5x5 tapered crystals + VPTs + HV filter

- 156 Supercrystals per **Dee**
- All crystals have identical dimensions
- All Supercrystals are identical (apart from inner and outer circumference)

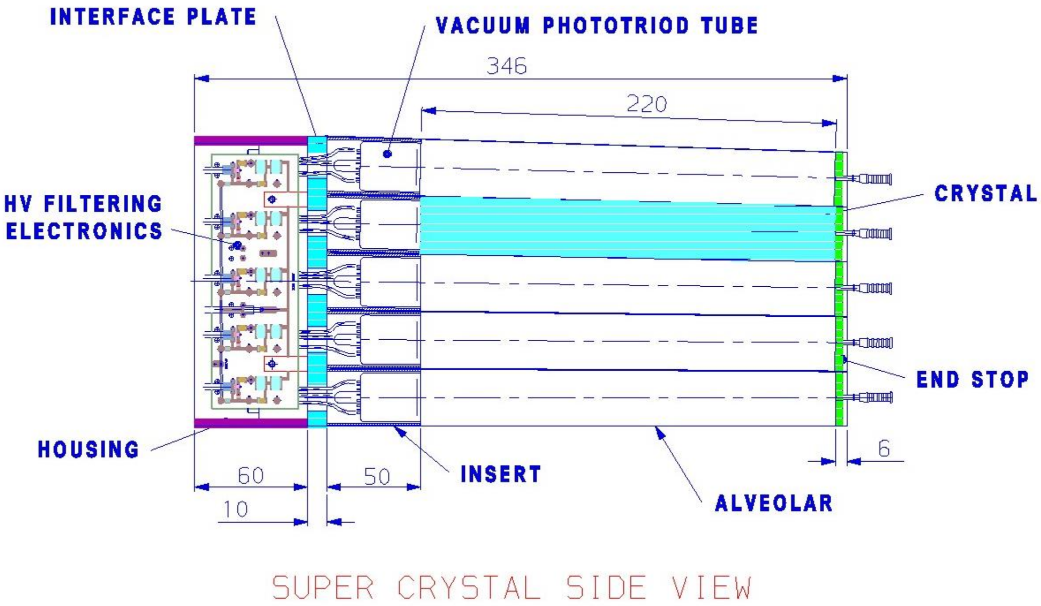

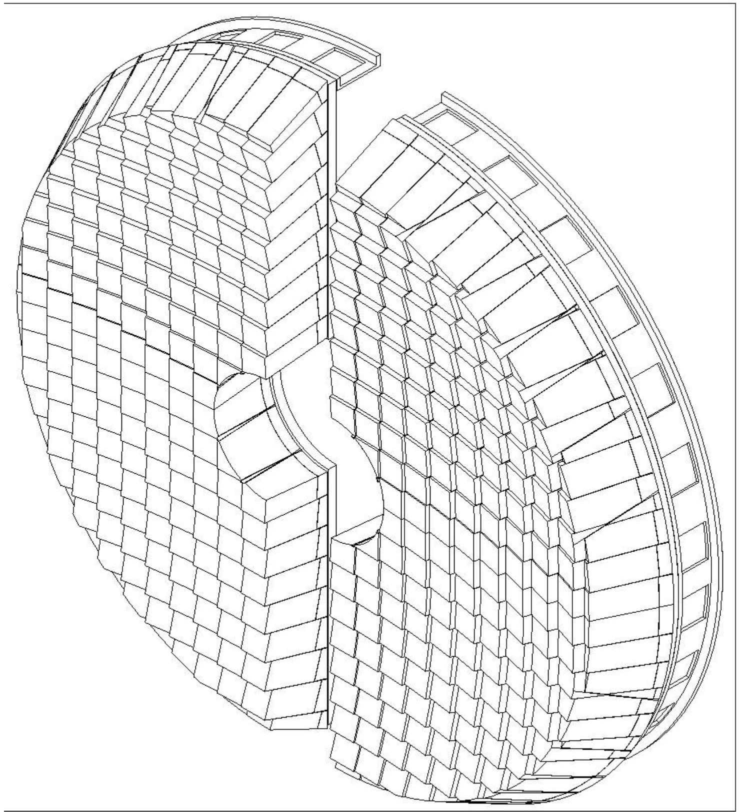

Evaluation of endcap crystals

Crystal lab at ICSTM has studied in detail the formation and annealing of colour centres

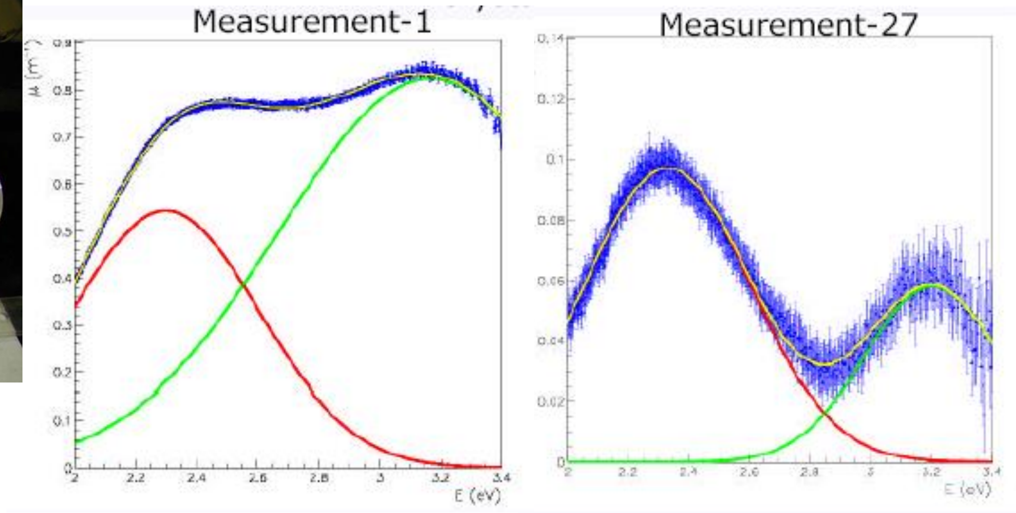

Ongoing developments have progressively increased the boule diameter:

Two barrel crystals are now cut from a single boule in current production

Even larger boules have been grown which could provide four crystals per boule

•Transmission loss due to irradiation at 15 Gy/h for 24 hours.

•Induced absorption fitted with Gaussians at 2.3 eV (540nm) and 3.1 eV (400nm).

Preshower detector

Rapidity coverage: 1.65 < |η| < 2.6 (End caps)

Motivation: Improved π^0/γ discrimination

- 2 orthogonal planes of Si strip detectors behind 2 X_0 and 1 X_0 Pb respectively
- Strip pitch: 1.9 mm (60 mm long)
- Area: 16.5 m^2 (4300 detectors, 1.4×10^5 channels)

Incident → Direction

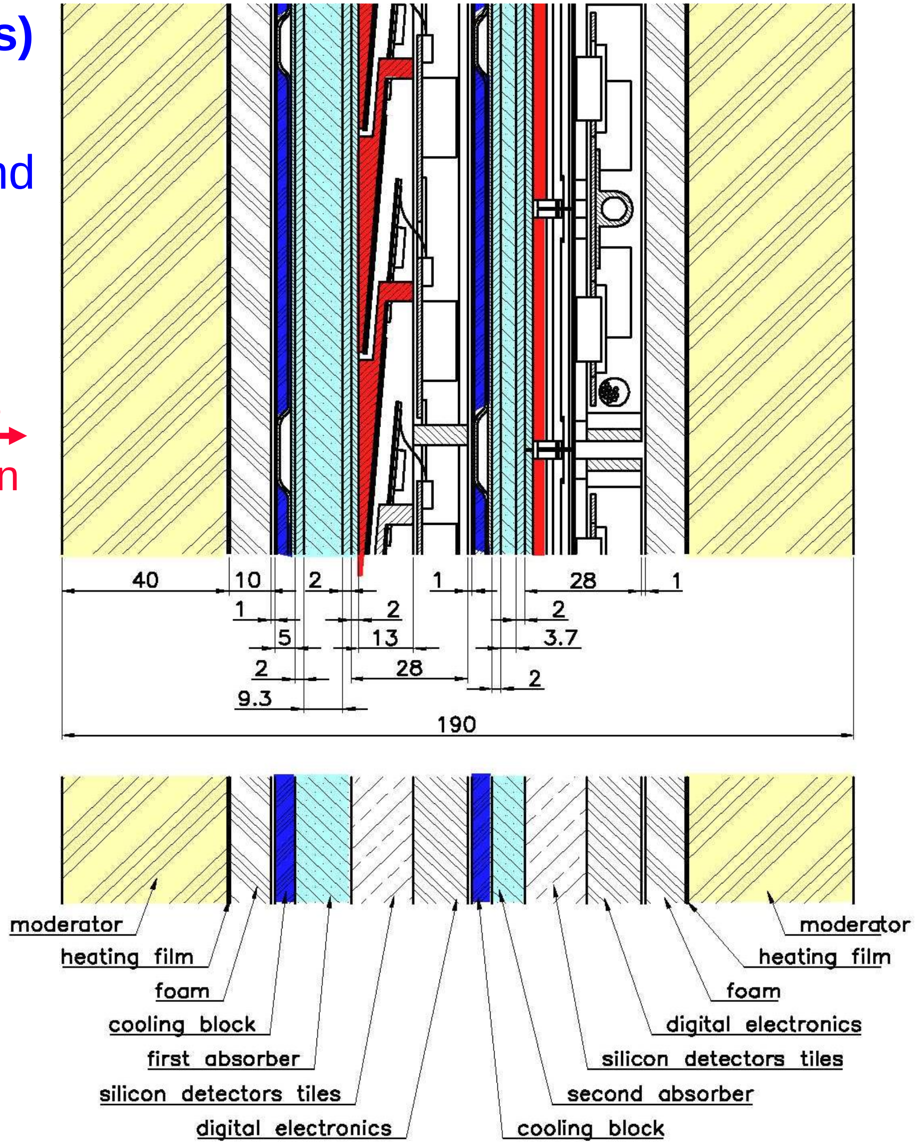

High radiation levels - Dose after 10 years:

- ~ 2×10^{14} n/cm^2
- ~ 60 kGy

➔ **Operate at -10^{o}C**

π^0/γ Discrimination

Photon P_T from 110 GeV Higgs

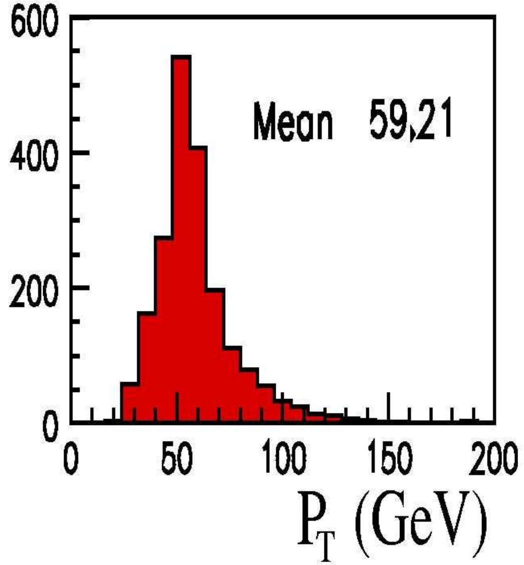

Barrel - use Crystals

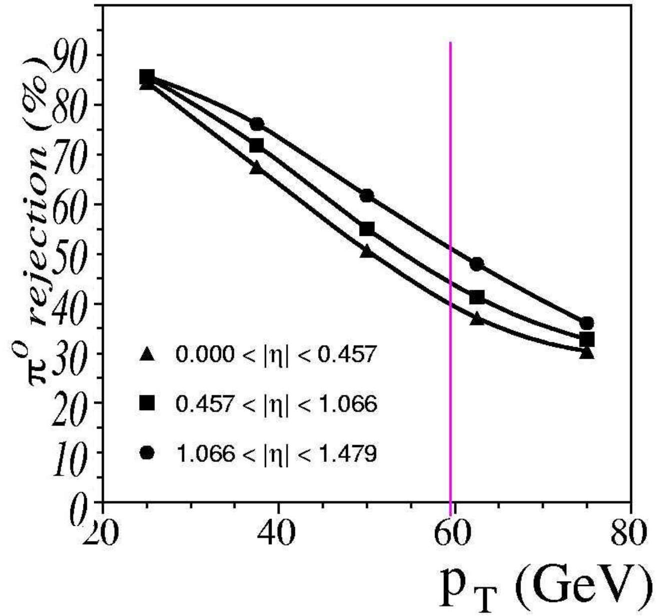

Endcaps - use Preshower

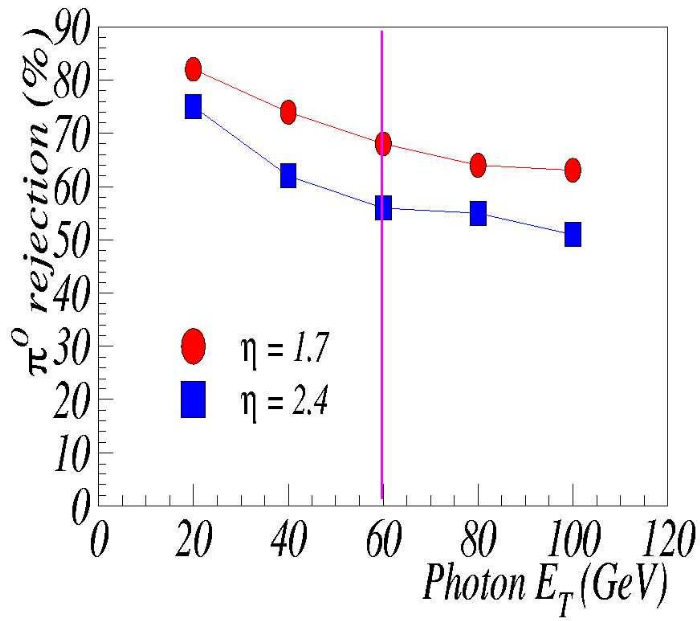

(γ-jet) is potentially the most serious background to $H \to \gamma\gamma$

Track isolation cut reduces (γ-jet) to ≈ 50% of the intrinsic (γ-γ) background (p_T cut = 2GeV/c)

Use π^0/γ discrimination in the ECAL to gain an extra margin of safety

Barrel: Lateral shower shape in crystals (limited by crystal size at high E_{π^0})

End cap: Cluster separation in preshower (limited by shower fluctuations at $3X_0$)

Test beam:Energy Resolution

Barrel - 3x3 crystals

$$\frac{\sigma_E}{E} = \frac{2.7\%}{\sqrt{E}} \oplus \frac{140\ \text{MeV}}{E} \oplus 0.4\%$$

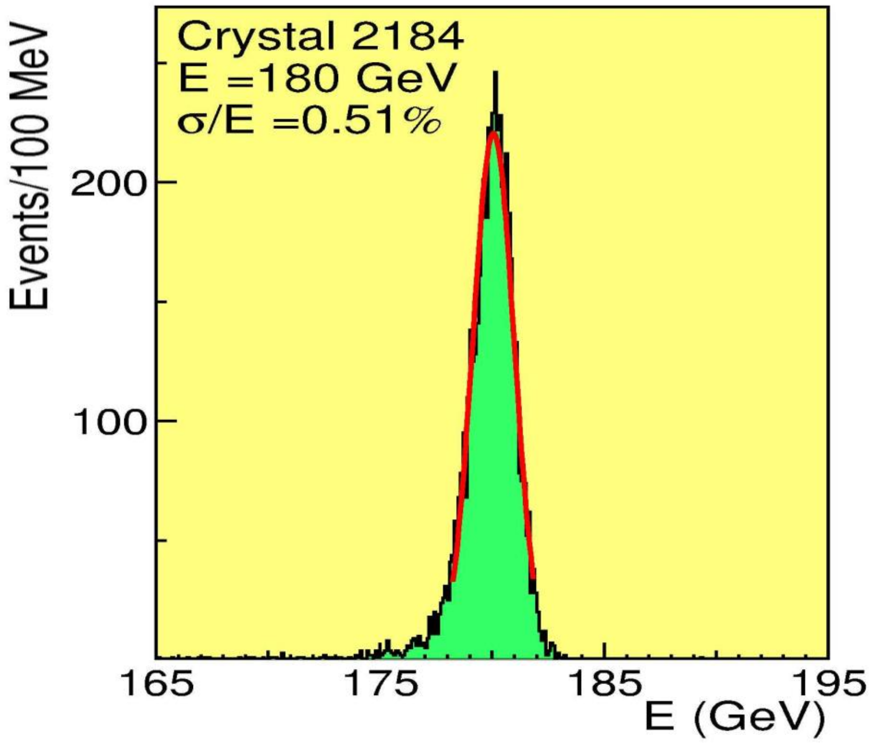

Endcap - 3x3 crystals

$$\frac{\sigma_E}{E} = \frac{4.1\%}{\sqrt{E}} \oplus \frac{140\ \text{MeV}}{E} \oplus 0.25\%$$

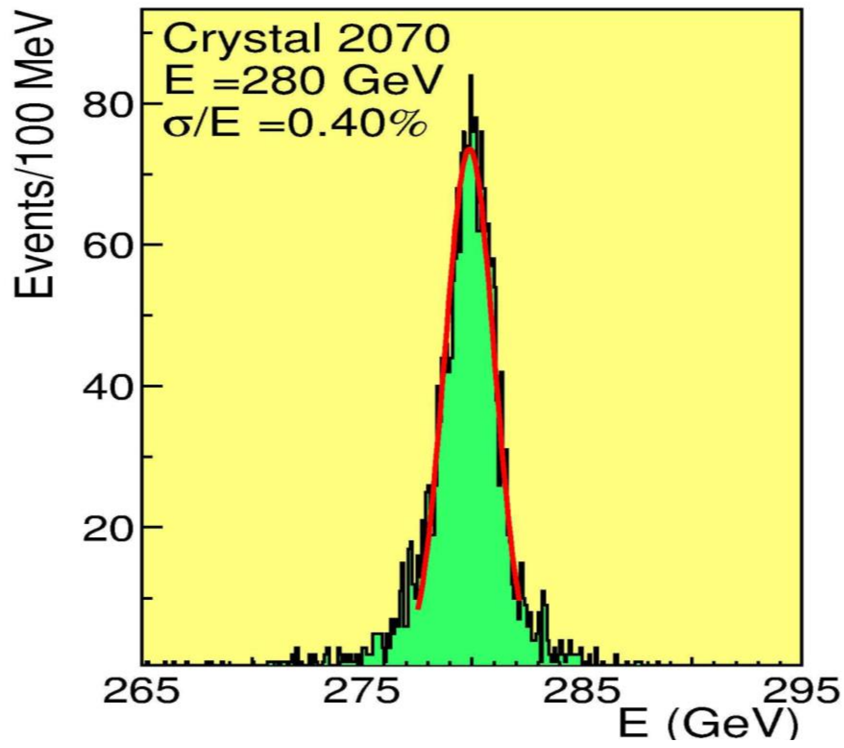

Barrel specifications: $$\frac{\sigma_E}{E} = \frac{2.7\%}{\sqrt{E}} \oplus \frac{155\ \text{MeV}}{E} \oplus 0.55\%$$

No preshower detector

Energy resolution with preshower

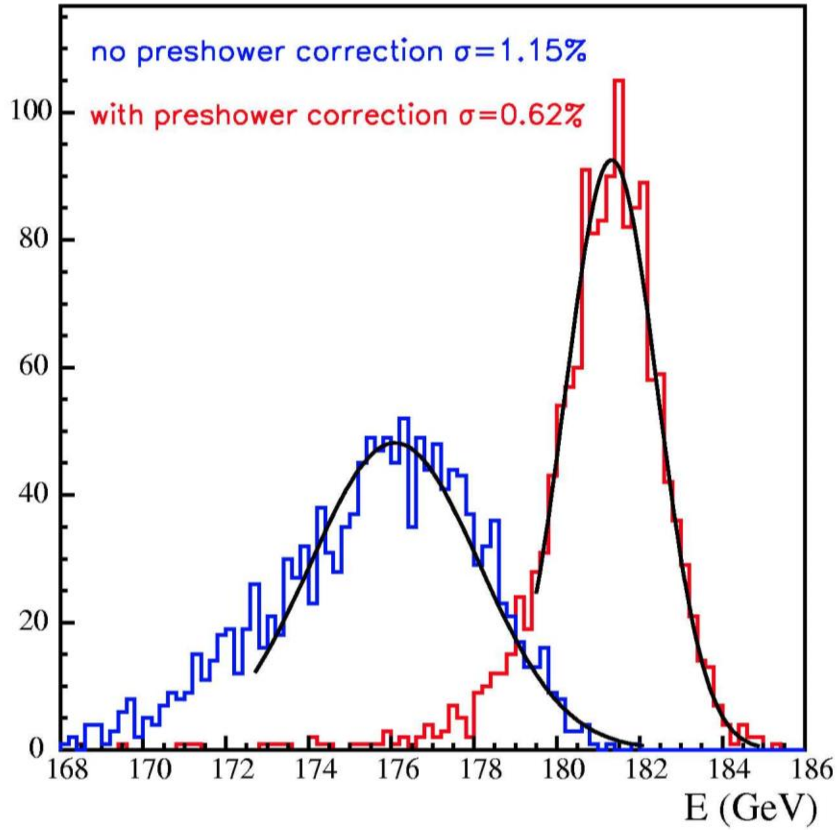

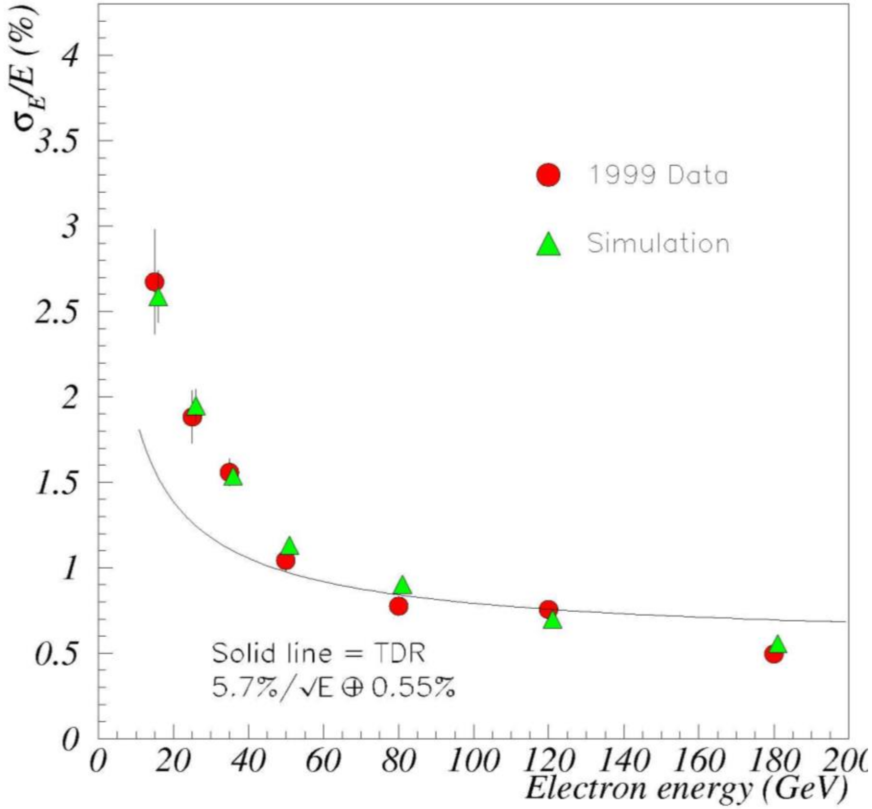

Energy resolution degraded by Pb absorber - partially restored using the Si-strip pulse-height information

Excellent agreement between MC and data

TDR performance achieved for E > 80 GeV ($\Rightarrow E_T > 30$ GeV - OK for H $\rightarrow \gamma\gamma$)

(even though Pb 10% too thick in this test!)

Laser Monitoring System

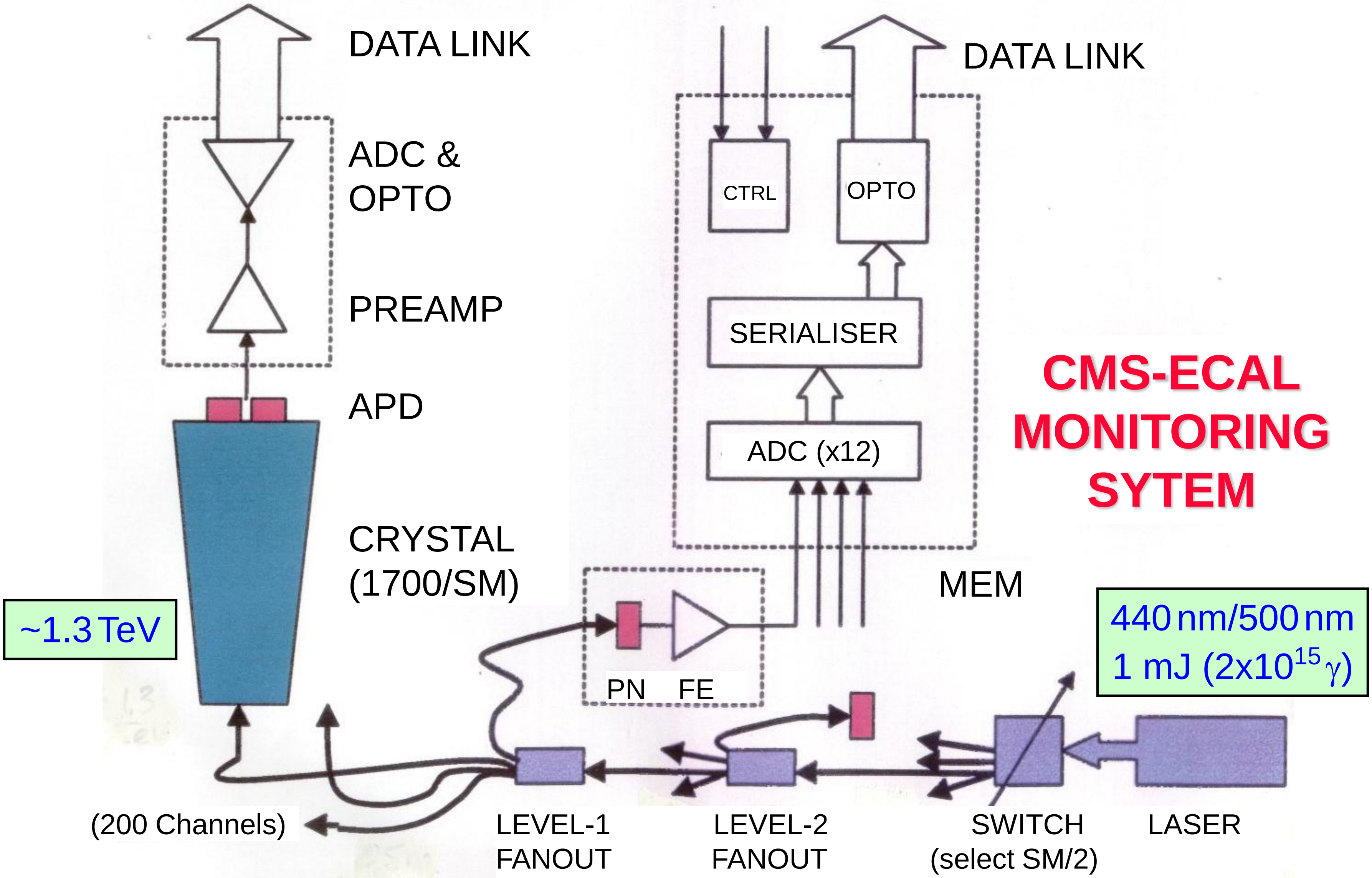

Laser Correction for Effect of Radiation Damage

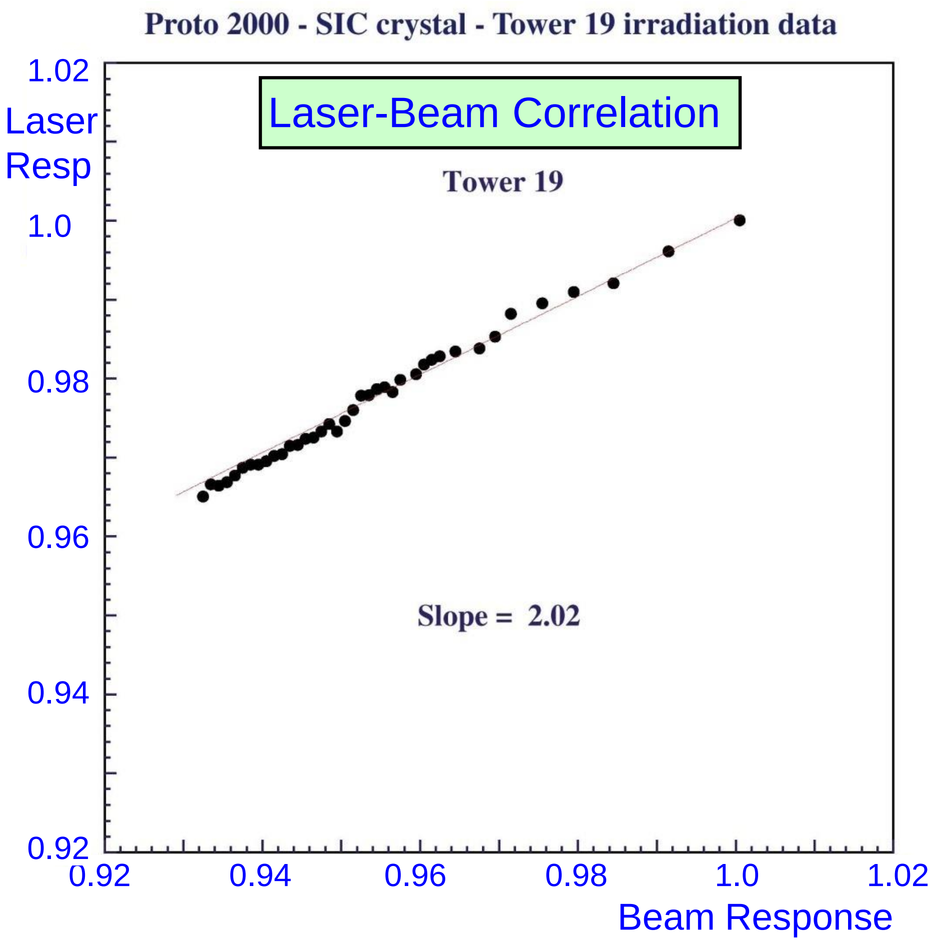

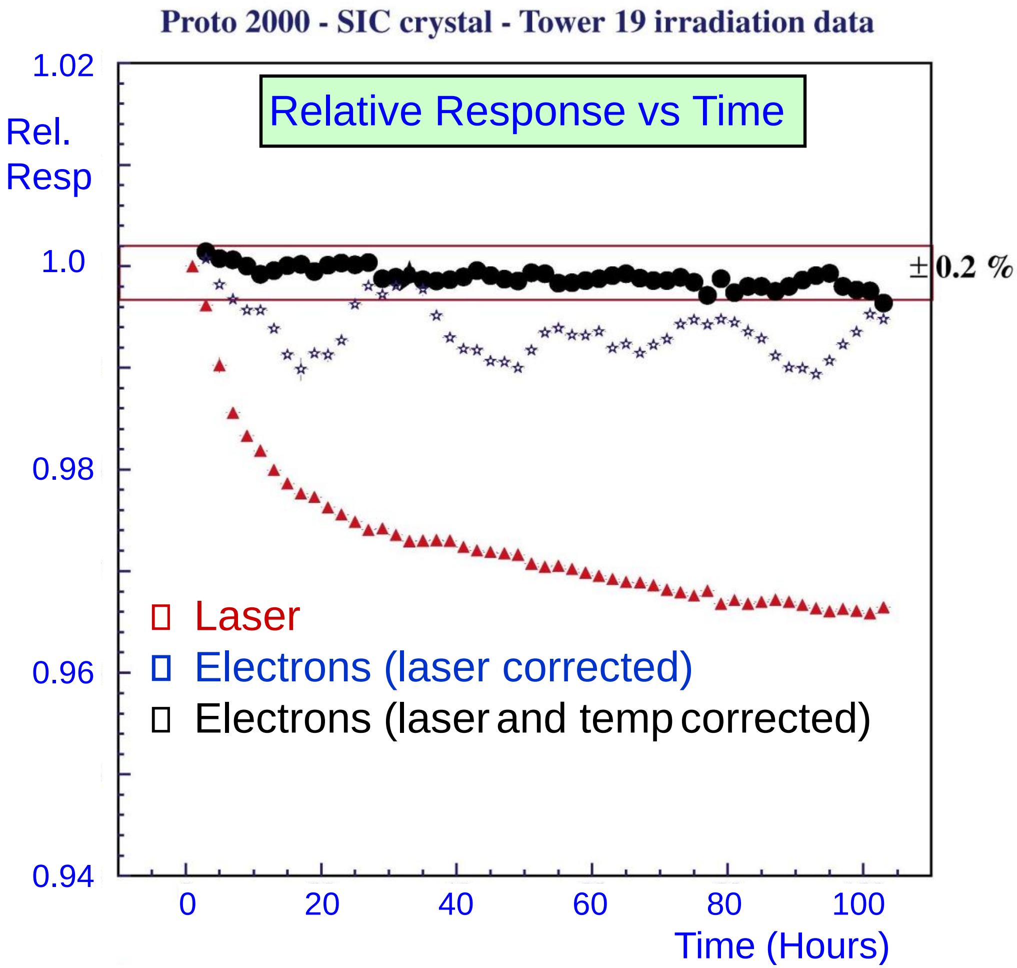

Readout architecture

Upper-level VME readout
(in Counting Room)

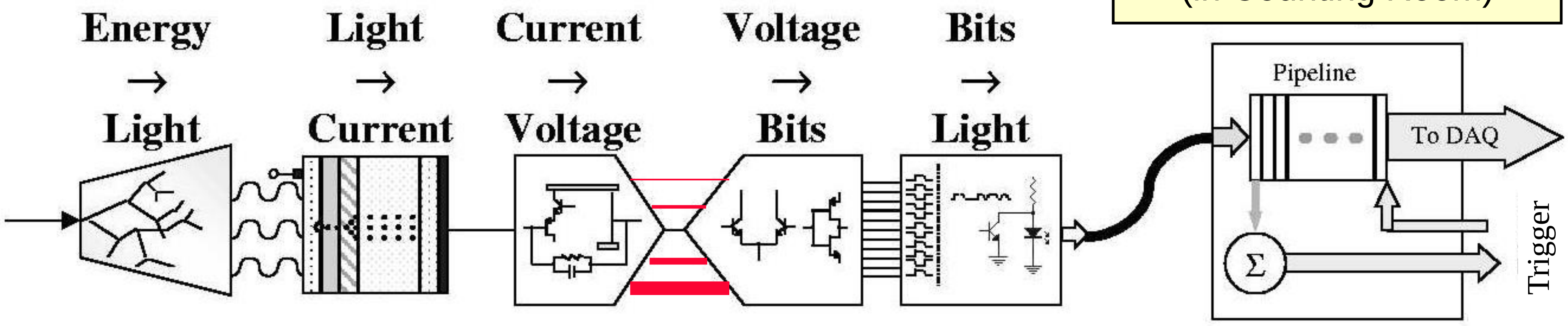

PbWO$_4$ Crystal | APD VPT | Preamp | Gain select | ADC | Serialiser + VCSEL | Optical link | Pipeline control, Interface → DAQ, Interface → Trigger

On-detector *light-to-light* readout

- 40 MHz Clock
- 12 bit precision
- 4 different gains ➔ >17 bit dynamic range

$PbWO_4$ Stopping Power

Validate ECAL calibration with muons: measure energy deposition vs muon momentum

momentum p measured in the CMS silicon tracker

dE: energy from ECAL cluster

dx: length traversed in ECAL crystals

dE/ρdx energy deposit matched to the track corrected for muon path length

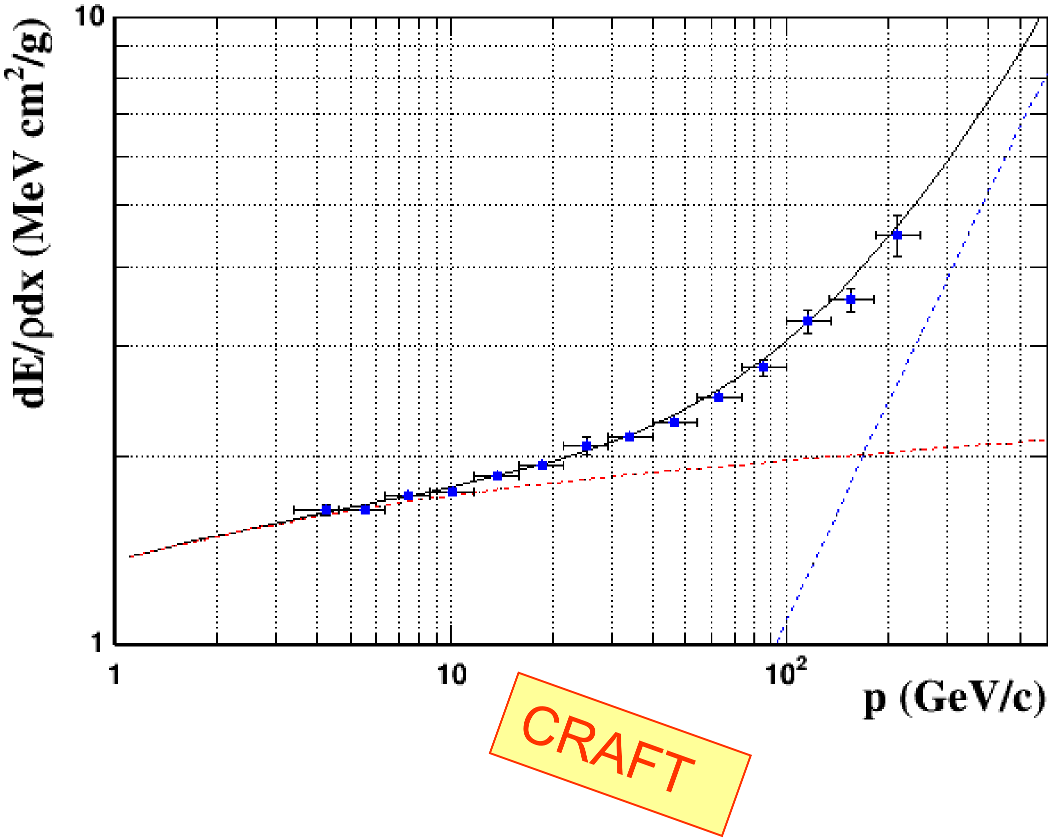

Tracker momentum matches well with ECAL energy loss, energy scale is correct

From Biino at ICATPP11 2009

Neutral pions

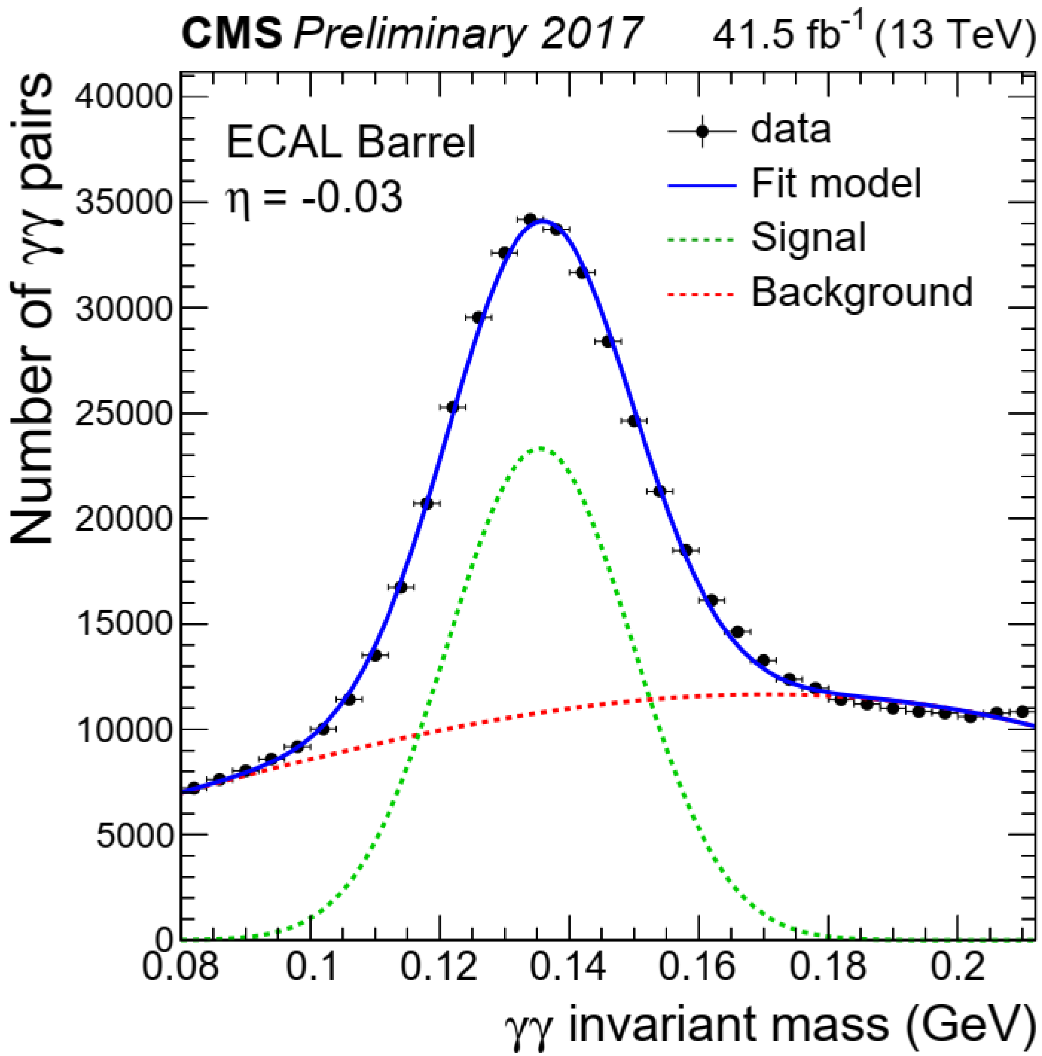

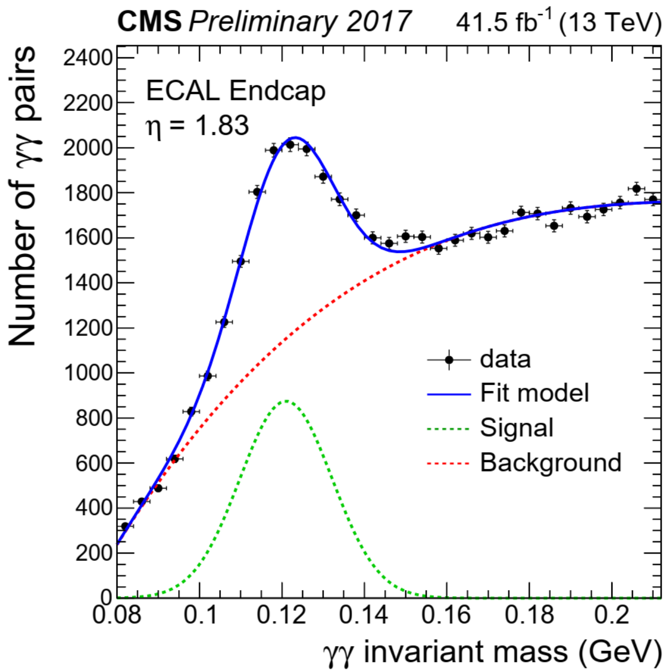

$\pi^0 \rightarrow \gamma\gamma$ where one of the two photons is reconstructed as a conversion

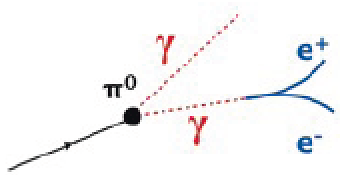

Intercalibration

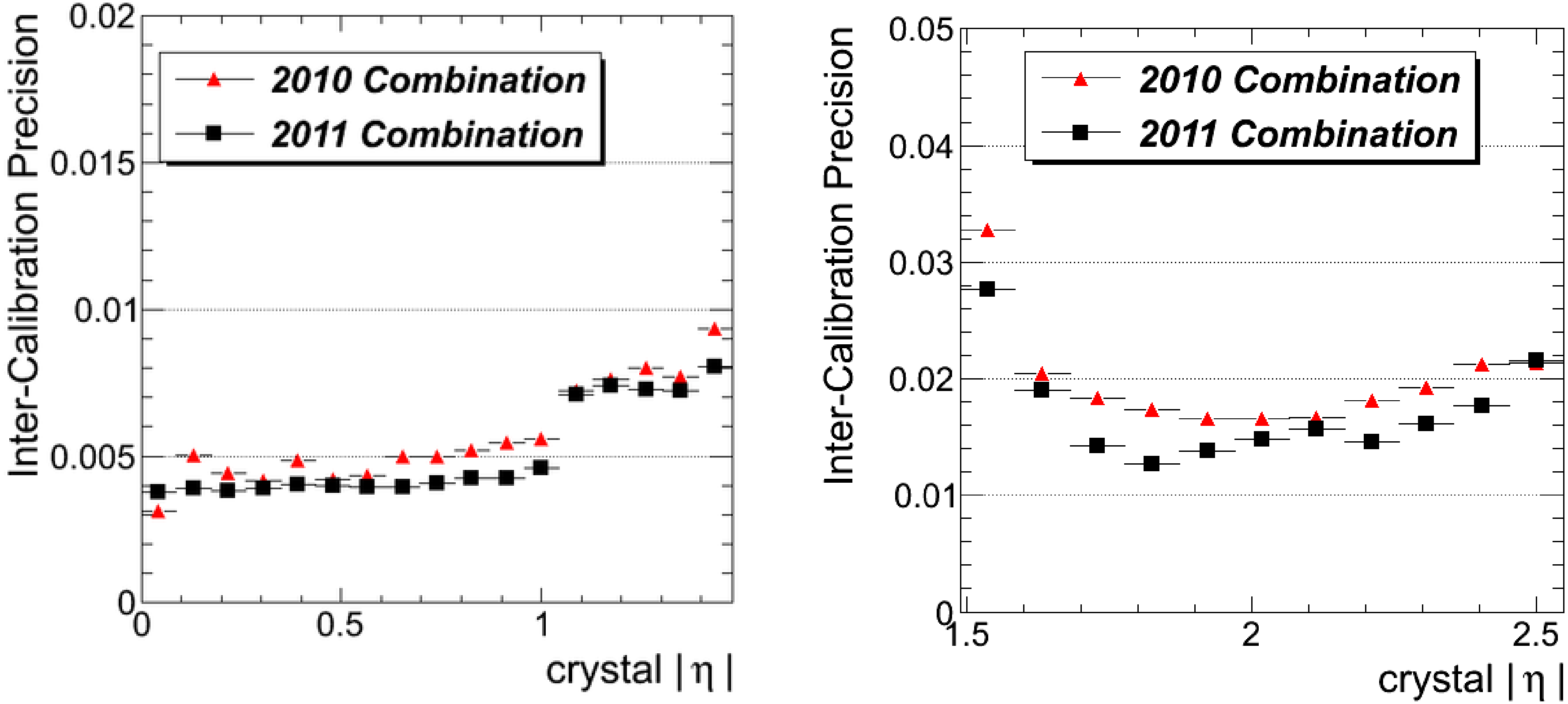

The precision of channel inter-calibration, using energy deposits, as a function of pseudo-rapidity in the ECAL barrel (left) and endcap (right) detectors

LHC radiation damage

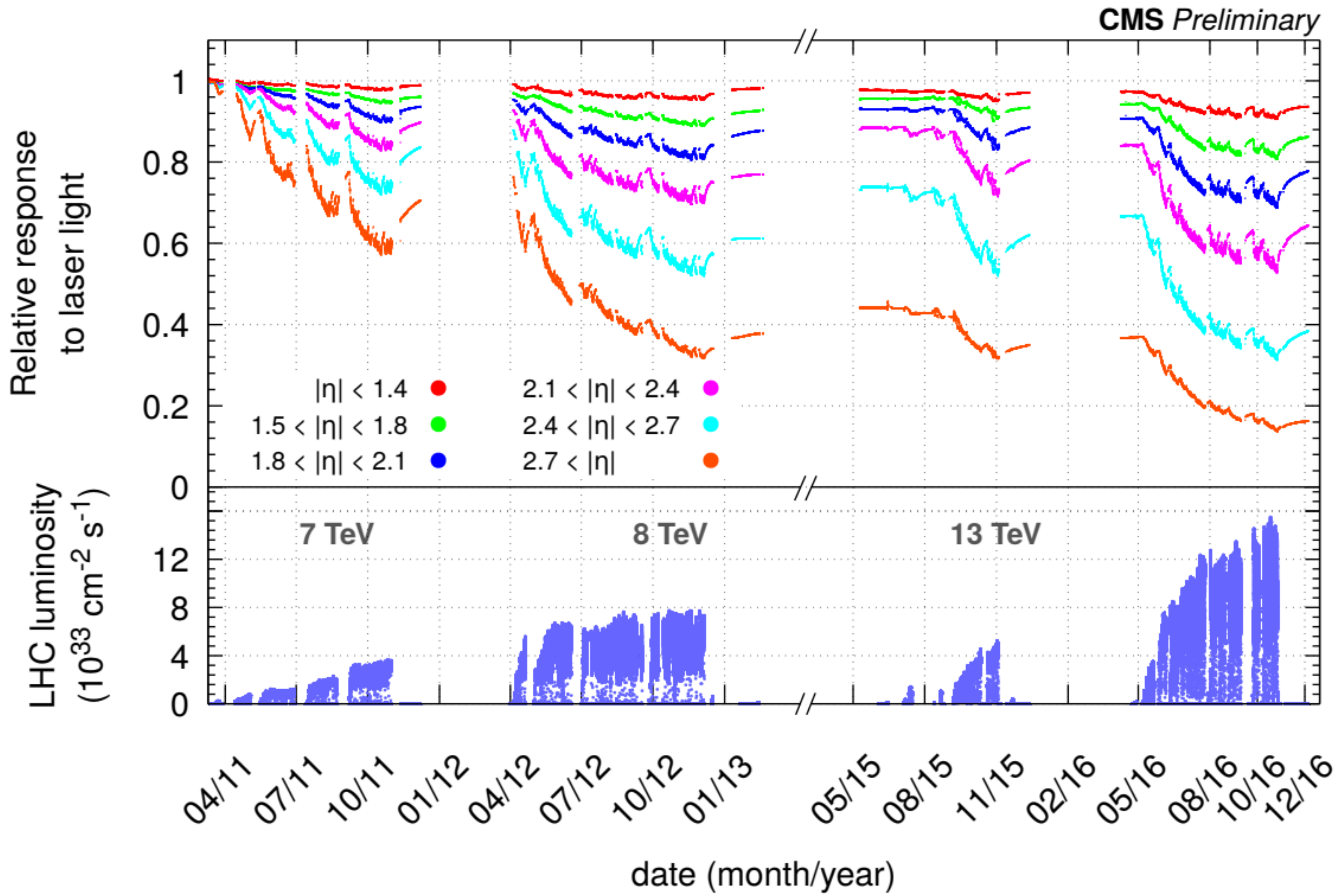

Relative response to laser light (440 nm) measured by the laser monitoring system, averaged over all crystals in bins of pseudorapidity, for the 2011 through 2016 data taking periods

LHC radiation damage

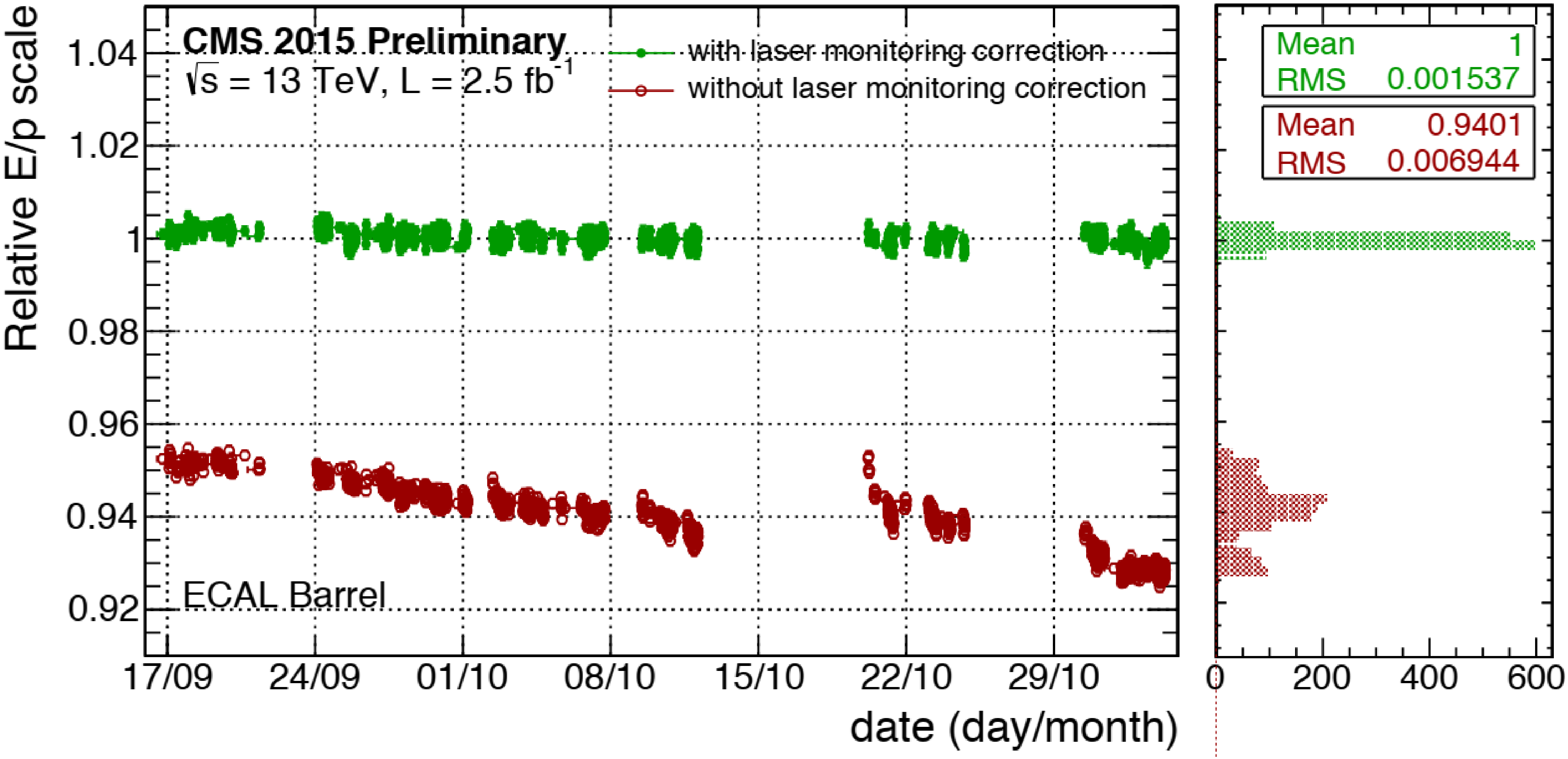

Correcting for the effects of radiation damage using the laser monitoring system. Barrel calorimeter shown here. In 2015 the average signal loss ~6% for ECAL Barrel, rms stability *after corrections* was 0.14%

The corrections work

Instrumental resolution in barrel is 1 GeV at the Z peak

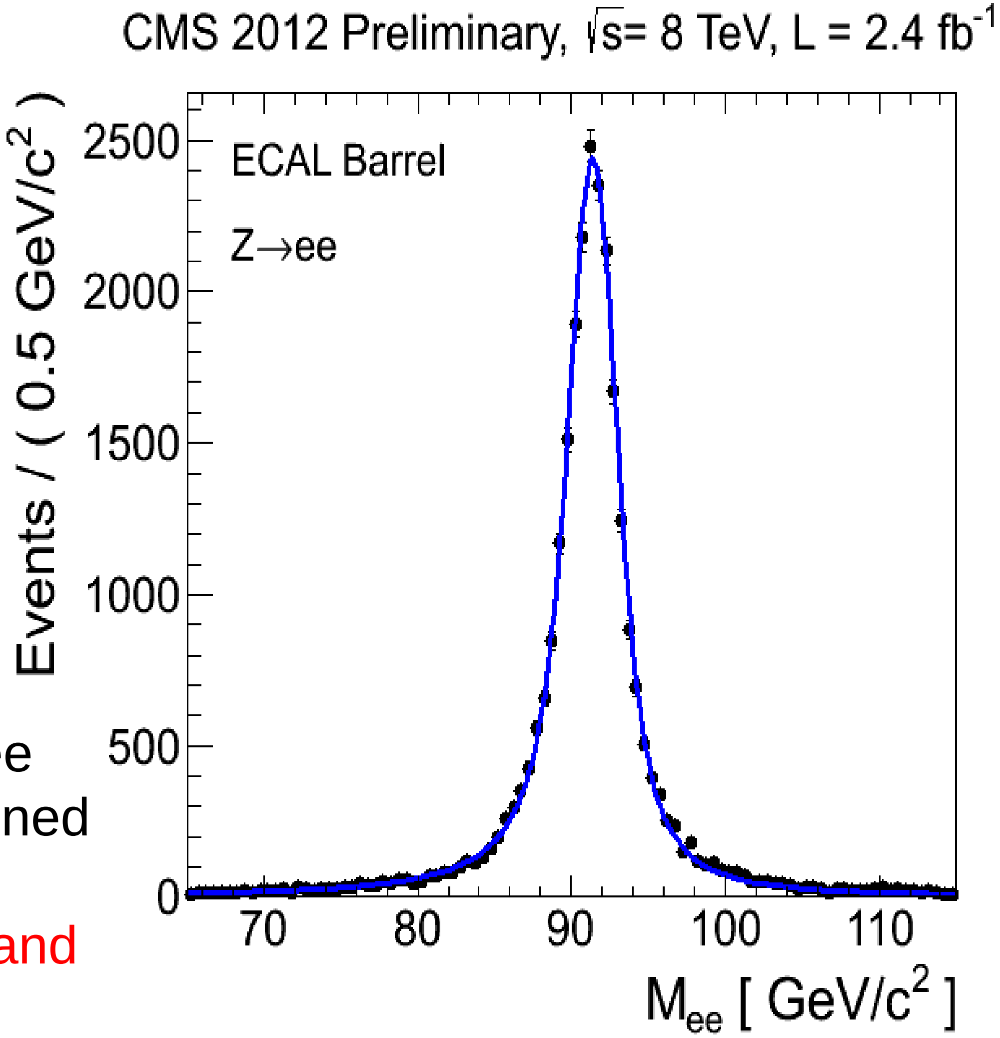

The plot shows the improvements in Z->ee energy scale and resolution that are obtained from applying energy scale corrections to account for the intrinsic spread in crystal and photo-detector response, and time-dependent corrections to compensate for crystal transparency loss

13 TeV operation

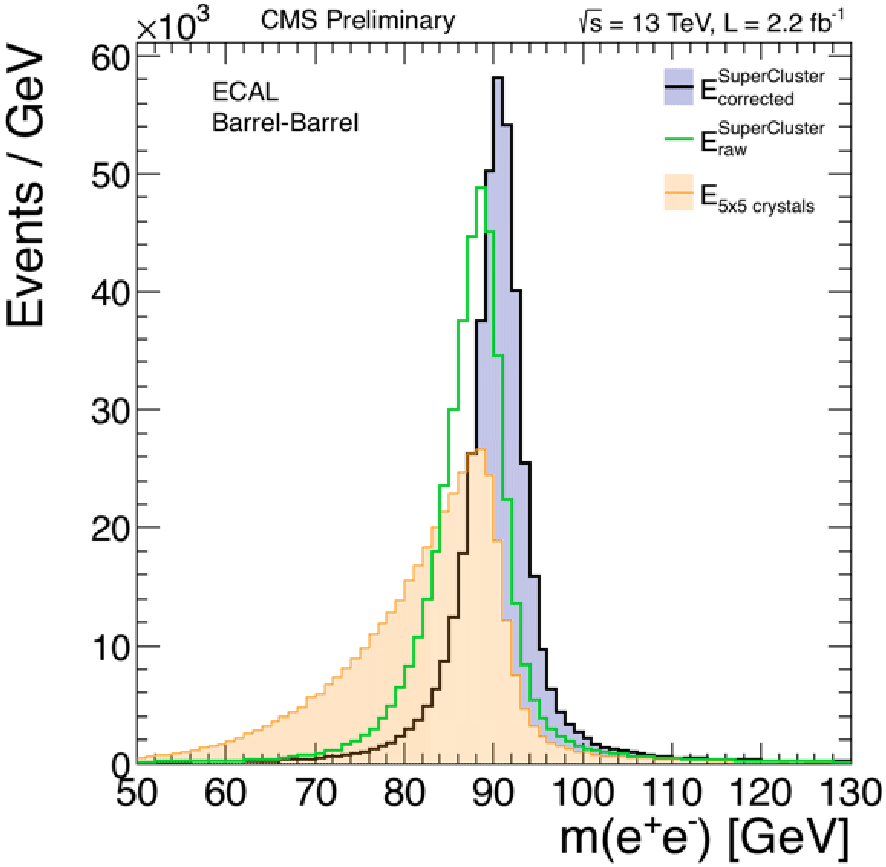

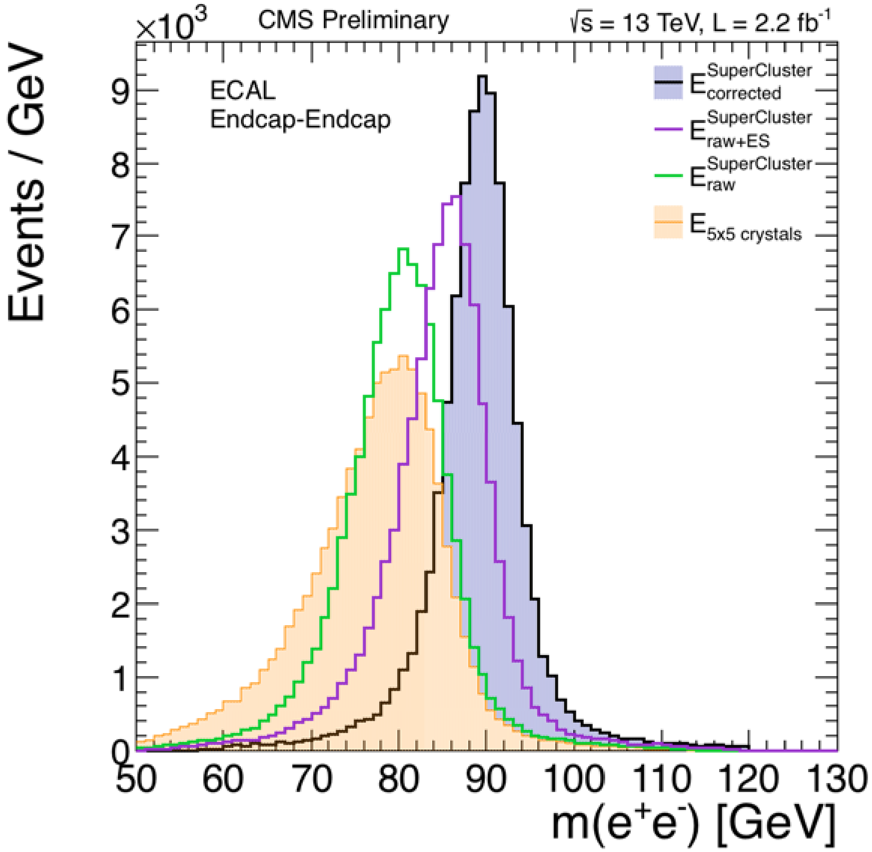

The two plots show the improvements to the $Z \rightarrow e^+e^-$ energy scale and resolution from the incorporation of more sophisticated clustering and cluster correction algorithms (energy sum over the seed 5x5 crystal matrix, bremsstrahlung recovery using supercluster, inclusion of preshower (ES) energy, energy correction using a multivariate algorithm).

13 TeV operation

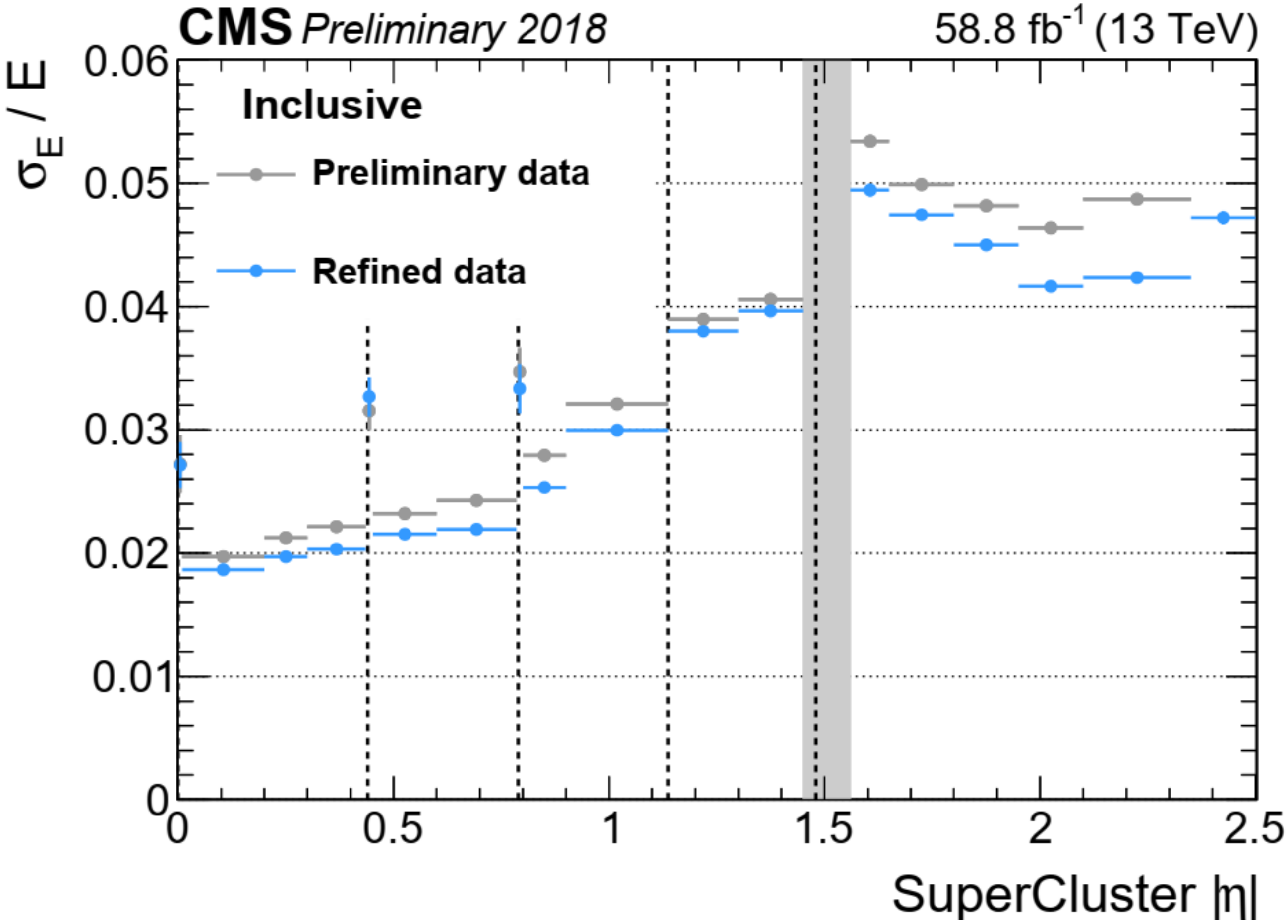

The plot shows the $Z \rightarrow e^+e^-$ energy resolution The region with the vertical grey bar is the physical join between the barrel and the endcap region.